Testing gravity with LSST

South American Workshop on Cosmology in the LSST Era

Nelson Padilla (PUC Chile)
www.astro.puc.cl/~npadilla
@ndpprocs

CONICET

Marie Sklodowska Curie
PCN - Horizon2020

The SHED collaboration

Nelson Padilla, Joaquin Armijo, Enrique Paillas (Santiago)
Sownak Bose (Harvard)
Yan-Chuan Cai, Andy Taylor, John Peacock (Edinburgh),
Baojiu Li, Marius Cautun (Durham, UK)

AIUC
CENTRO DE ASTRO-INGENIERIA UC

CONICYT
Ministerio de Educación
Gobierno de Chile

LSST DESC
Dark Energy Science Collaboration

Outline

- Cold dark matter with and without a cosmological constant: GR vs. MoG.
- GR, f(R) and nDGP simulations
- Equal clustering and CMB for all models.
- Marked correlation functions and weak lensing around voids: probes of gravity for LSST
- Signatures from different screening mechanisms

General Relativity

dark energy 70%

Lambda Cold Dark Matter

Cosmology

dark matter 25%

Baryons 5%

How about Modifying Gravity?

MoG: no dark energy

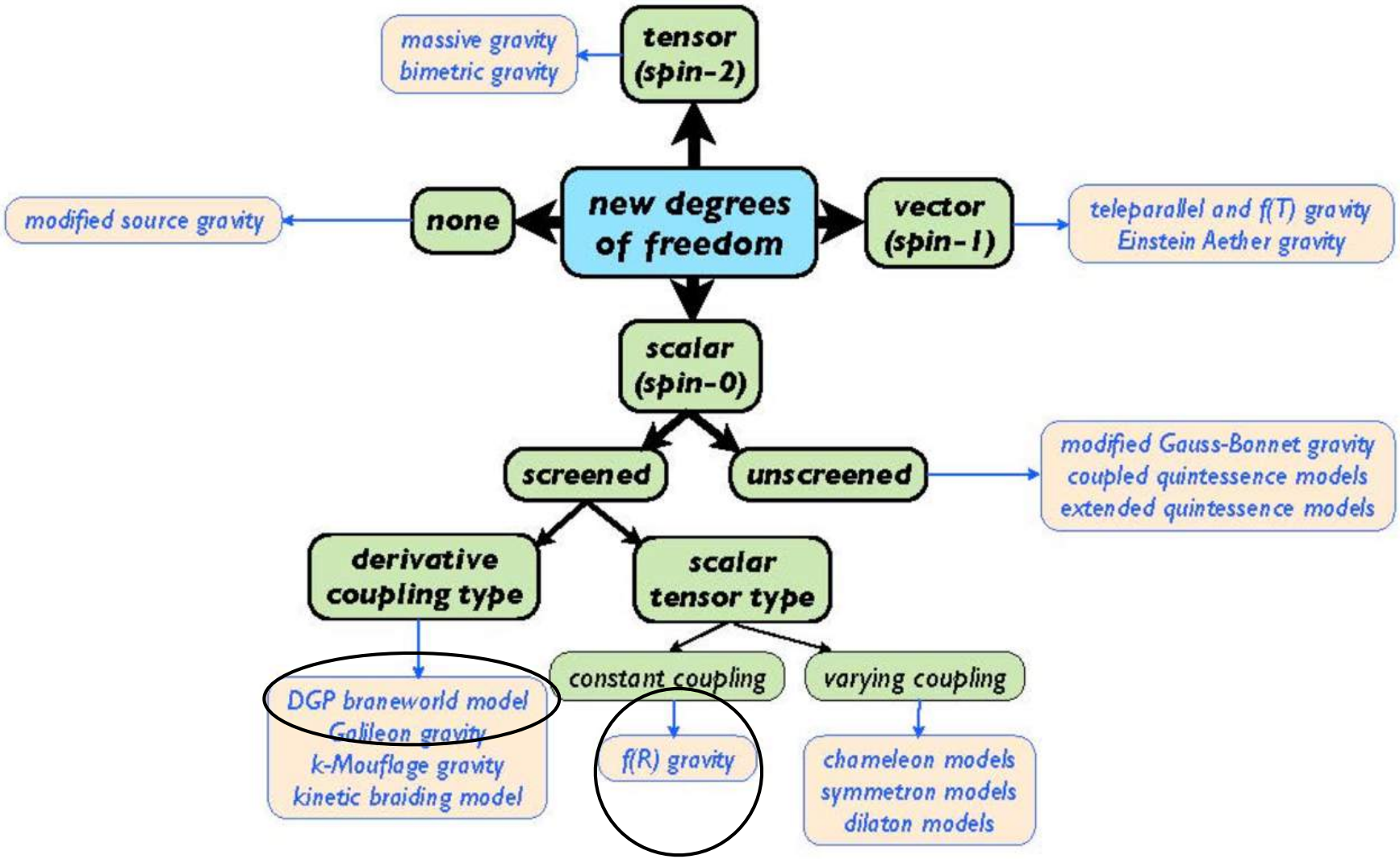

Courtesy Baojiu Li

MoG

- Modified gravity (MoG) models can explain the accelerating expansion without a cosmological constant.
- Scalar field coupled to matter or extra term in Einstein-Hilbert action trigger extra fifth force that enhances gravity.
- Screening mechanism (Chameleon in f(R), Vainshtein in nDGP) that suppresses fifth force in high density regions is needed to make observationally viable theory.
- Fifth force is screened in early universe (CMB is unchanged) and in high density regions (Solar system).
- **Empty regions in space** would be the place to look for the fifth force.

Microwave background radiation points to LCDM
No need to simulate this, density contrast is linear.

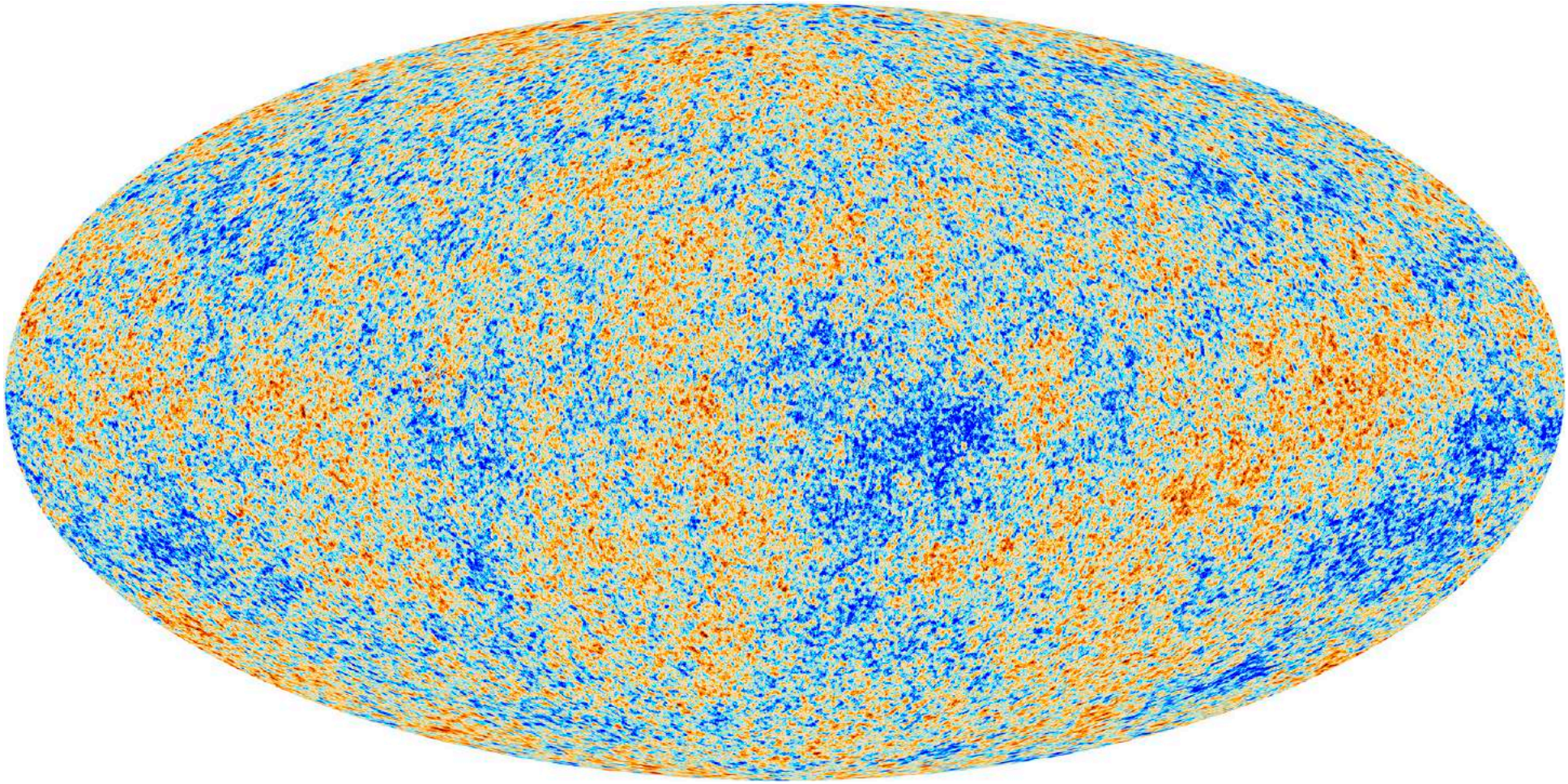

Image credit: Planck collaboration

Density map of z~0 Universe is highly non-linear.

It shows galaxies, not mass.

We have a good idea of how galaxies populate the dark matter field, but there is still freedom.

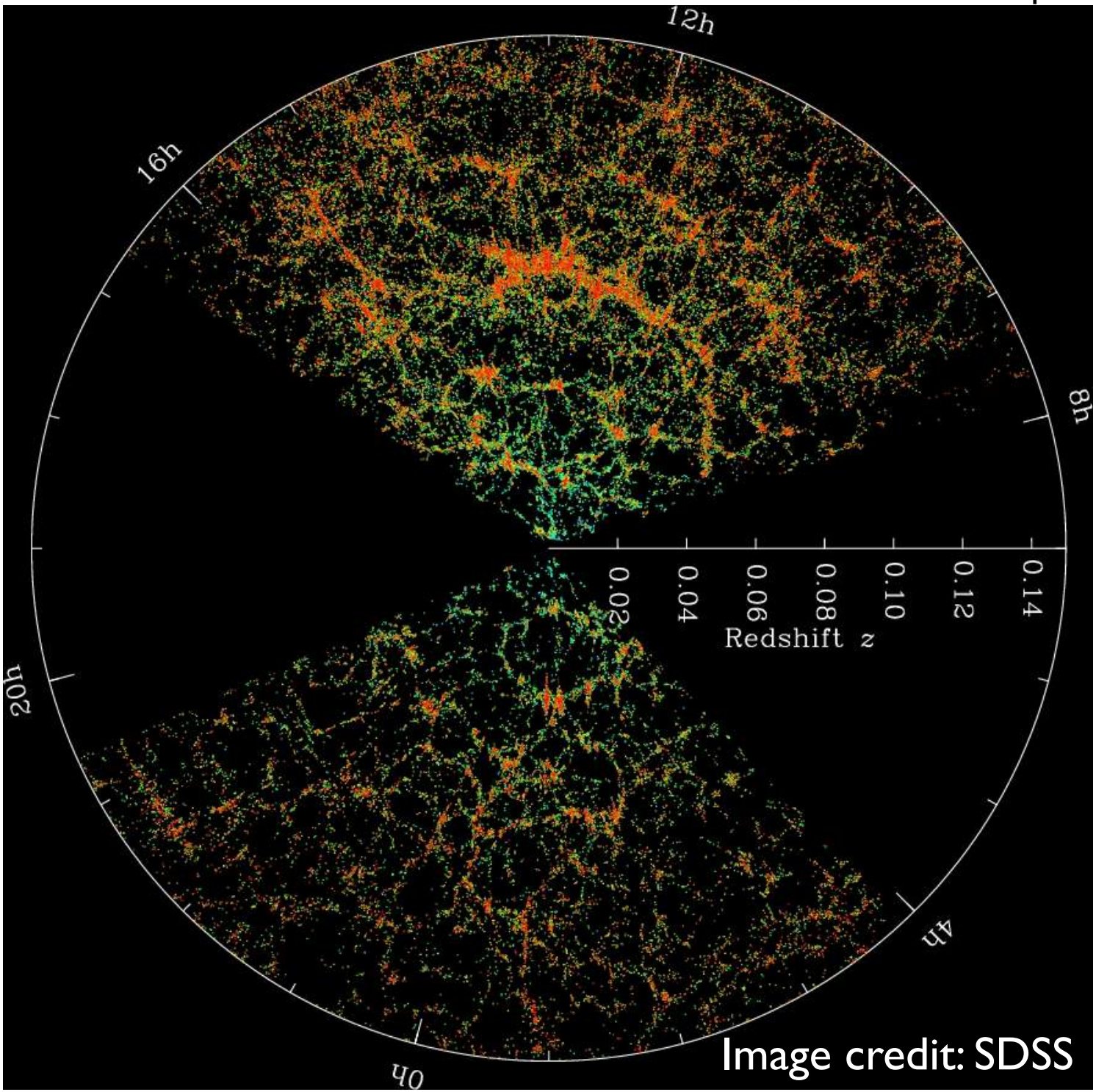

f(R) MOG

Replace cosmological constant by f(R) in the action:

$$S = \int \mathrm{d}^4x\sqrt{-g}\left[\frac{1}{2}M_{\mathrm{Pl}}^2\left(R+f(R)\right)+\mathcal{L}_{\mathrm{m}}\right]$$

where g is the determinant of the metric tensor, R is the Ricci scalar, M_{Pl} is the reduced Planck mass.

When the curvature is high f(R) approaches a constant (and behaves as a cosmological constant).

Other regimes: complicated dynamics and rich phenomenology with eq. of motion from trace of the modified Einstein equation (obtained by varying the Action):

$$\Box f_R = \frac{1}{3}\left[R - f_R R + 2f(R) + 8\pi G\rho_{\mathrm{m}}\right] \qquad f_R \equiv \mathrm{d}f(R)/\mathrm{d}R$$

In the limit $f_R \to 0$, $f(R) \to 2\Lambda$ so that $R = -8\pi G\rho_{\mathrm{m}} + 4\Lambda$, the first condition for viable f(R)

In order to pass Solar System checks: $f_R \to 0$ when $\rho_{\mathrm{m}} \to \infty$

The Hu & Sawicky model satisfies this condition and f(R) is constant in the background throughout cosmic history.

f(R) MOG

In the regime of slow time variation for fluctuations with respect to background, and negligible kinetic energy for the field

Modified Poisson Equation:

$$\vec{\nabla}^2\Phi = \frac{16\pi G}{3}a^2\left(\rho_m - \bar{\rho}_m\right) + \frac{1}{6}a^2\left[R\left(f_R\right) - \bar{R}\right]$$

$$\nabla^2 f_R = -\frac{1}{3}a^2\left[R(f_R) - \bar{R} + 8\pi G\left(\rho_{\rm m} - \bar{\rho}_{\rm m}\right)\right]$$

Hu-Sawicky f(R) model:

$$f(R) = -M^2\frac{c_1\left(-R/M^2\right)^n}{c_2\left(-R/M^2\right)^n + 1}$$

where

$$\frac{c_1}{c_2^2} = -\frac{1}{n}\left[3\left(1 + 4\frac{\Omega_\Lambda}{\Omega_{\rm m}}\right)\right]^{1+n} f_{R0}$$

and the characteristic mass M satisfies $M^2 = 8\pi G\bar{\rho}_{\rm m0}/3 = H_0^2\Omega_{\rm m}$

Cluster abundance data constrain: $|f_{R0}| \lesssim 10^{-4}$ for n=1 (Schmidt et al. 2009).
This is the chameleon parameter.

Also with other observables: Jennings et al. (2012), Hellwing et al. (2013)

f(R) predictions using spherical top-hat model

Haloes and the fifth force

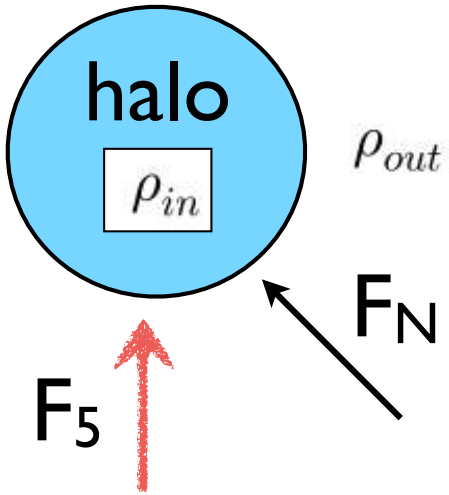

- Positive fifth force outside haloes acting in addition to newtonian.
- Effect present at low masses.
- At high masses effect increases for high fifth force strength parameter.

f(R) predictions using spherical top-hat model

- Clampitt et al. 2013 calculate the fifth and newtonian forces for a top-hat empty region (**voids**).

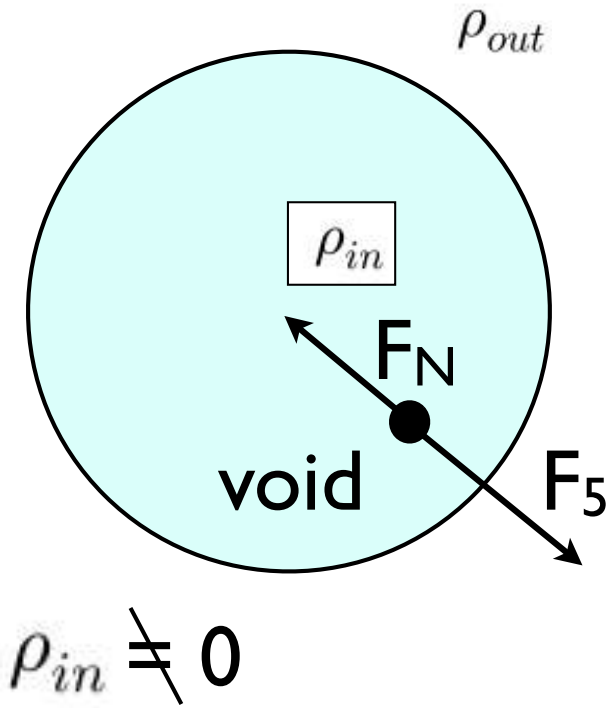

Negative fifth force inside voids acting in opposite direct-ion to newtonian. Stronger for lower internal density, and for small voids.

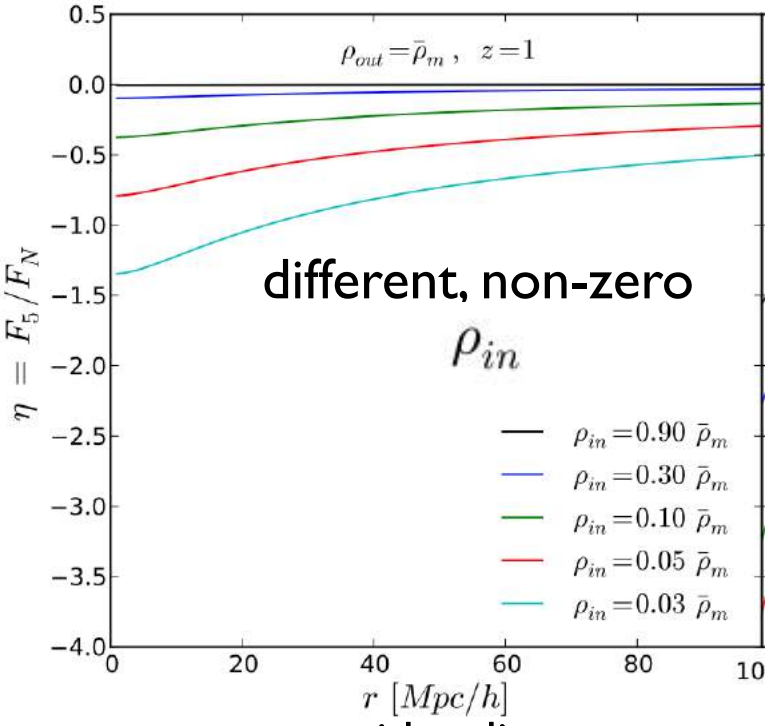

nDGP gravity

- Normal branch of the 5D Dvali-Gabadadze-Porrati (Dvali+2000)

$$S = \int_{\text{bulk}} \mathrm{d}^5x\, \sqrt{-g^{(5)}}\, \frac{R^{(5)}}{16\pi G^{(5)}} + \int_{\text{brane}} \mathrm{d}^4x\, \sqrt{-g}\, \frac{R}{16\pi G}$$

- Modified gravity with Vainshtein screening mechanism (k-mouflage, Vainshtein 1972)
- Additional dark energy component provides accelerated expansion (not needed in sDGP)
- Gravity felt by massive particles includes 5-th force mediated by scalar field
- Extra parameter: $r_c = \frac{1}{2}\frac{G^{(5)}}{G}$

nDGP gravity

- Modified Poisson equation

$$\nabla^2\Phi = 4\pi G a^2 \left(1 + \frac{1}{3\beta(a)}\right)\delta\rho$$

where the strength of the fifth force is given by

$$\begin{aligned}\beta(a) &= 1 + 2Hr_c\left(1 + \frac{\dot{H}}{3H^2}\right) \\ &= 1 + \left[\frac{\Omega_{m0}a^{-3} + \Omega_{\Lambda 0}}{\Omega_{rc}}\right]^{1/2} - \frac{1}{2}\frac{\Omega_{m0}a^{-3}}{\sqrt{\Omega_{m0}a^{-3} + \Omega_{\Lambda 0}}}\end{aligned}$$

Spherical solution provides estimate of Vainshtein screening radius,

$$r_V^3 \equiv \frac{8r_c^2 r_S}{9\beta^2} \equiv \frac{4GM}{9\beta^2 H_0^2 \Omega_{rc}} \qquad \Omega_{rc} = 1/(4H_0^2 r_c^2)$$

nDGP predictions using spherical model

Haloes and the fifth force

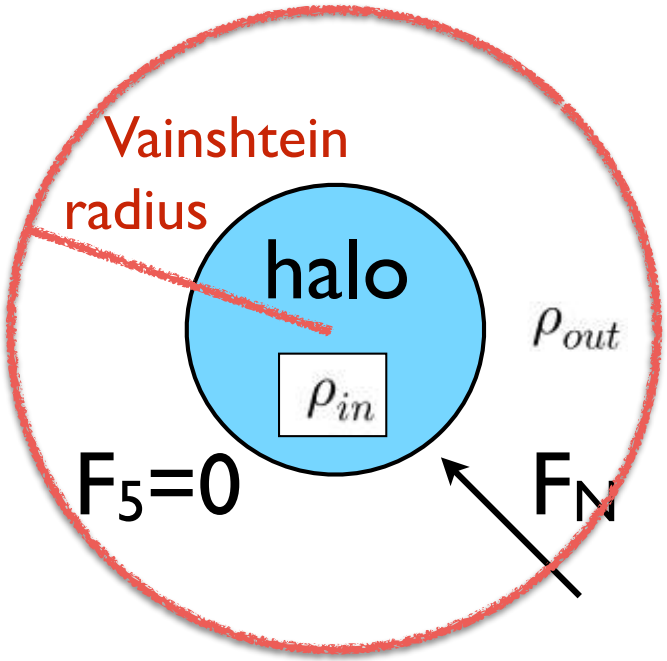

- Positive fifth force outside Vainshtein radius acting in addition to newtonian.
- Effect present at all masses.

nDGP predictions using ~spherical model

- In voids, Vainshtein radius removes the fifth-force around void haloes. Different phenomenology is expected.

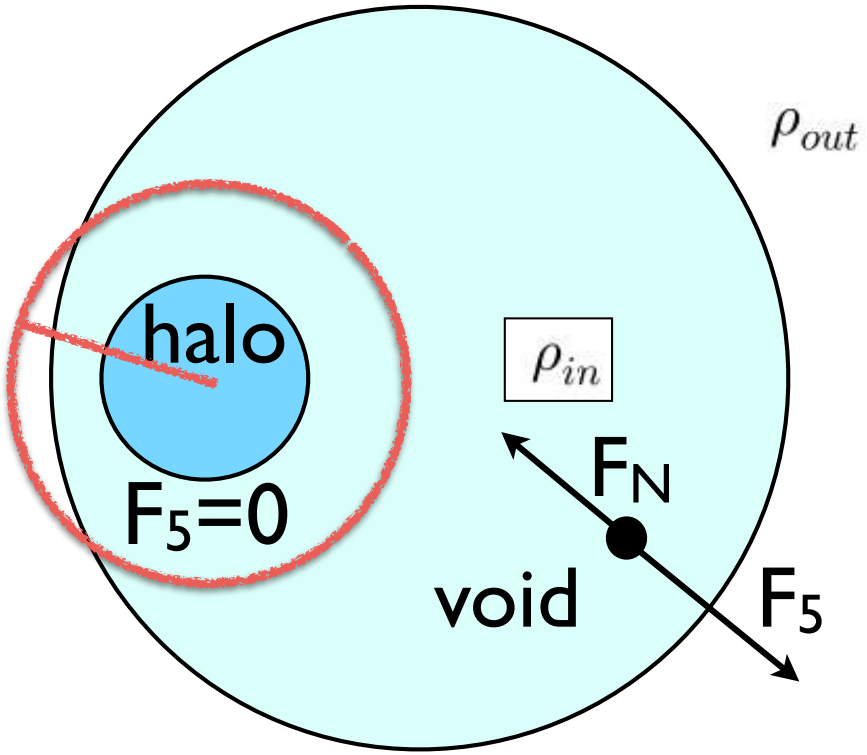

$\rho_{in} \neq 0$

Negative fifth force inside voids acting in opposite direct-ion to newtonian away from haloes. Stronger for lower internal density, and for small voids.
~Null inside Vainshtein radius.

Screening types differ

Fully non-linear solution for different screening types, with equal galaxy clustering.

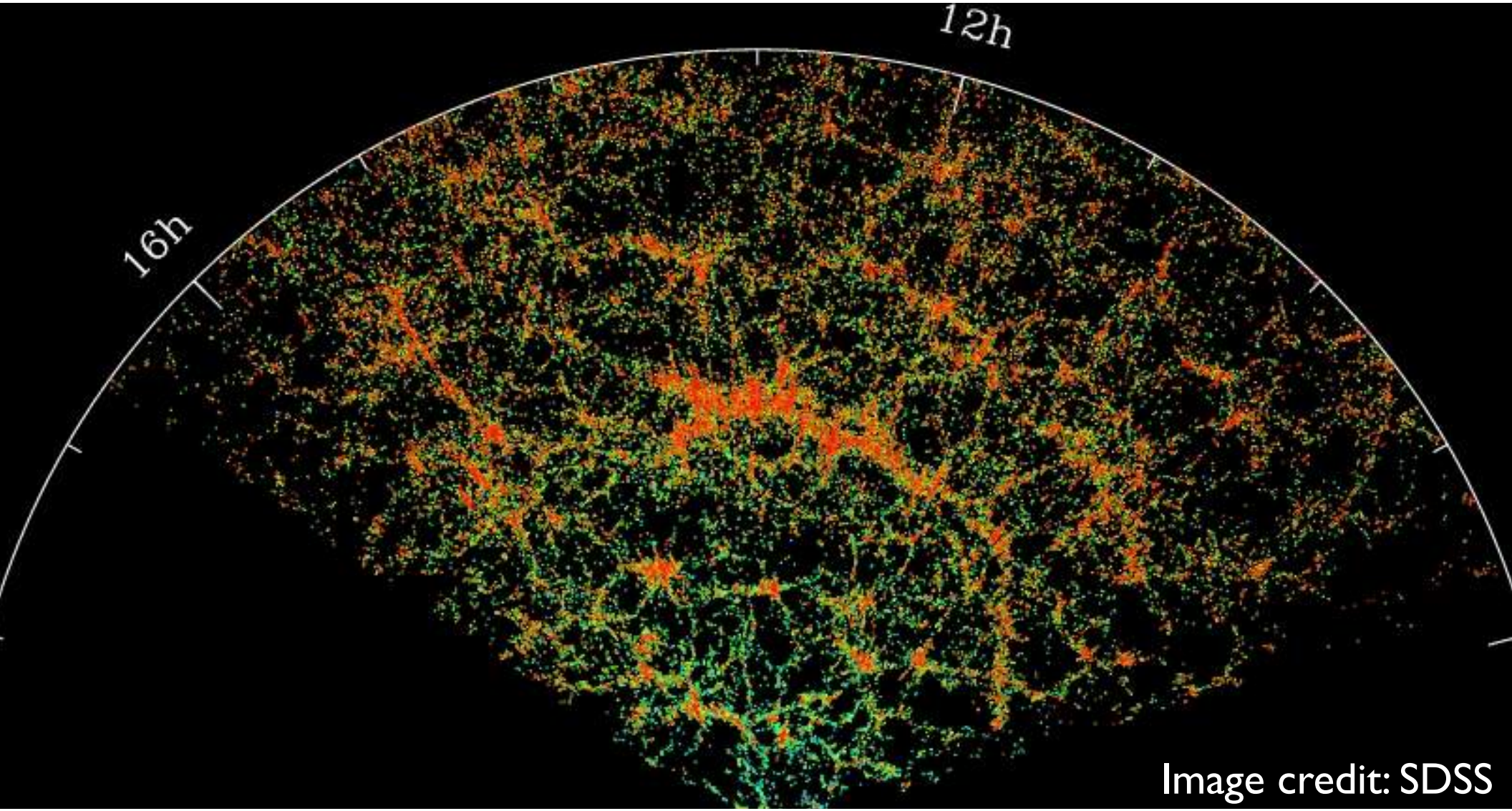

MoG simulations: chameleon model (f(R))

Modified Poisson equation and equation for f_R (Jennings et al. 2012):

$$\nabla^2 f_R = -\frac{1}{3}a^2\left[R(f_R) - \bar{R} + 8\pi G\left(\rho_{\rm m} - \bar{\rho}_{\rm m}\right)\right] \qquad \nabla^2\Phi = \frac{16\pi G}{3}a^2\left(\rho_{\rm m} - \bar{\rho}_{\rm m}\right) + \frac{1}{6}a^2\left[R\left(f_R\right) - \bar{R}\right]$$

Simulations from Zhao, Li & Koyama, 2012: ECOSMOG code (Li et al. 2012) based on RAMSES (Teyssier 2002)

GR and f(R) models start from the same initial conditions.

MoG simulations: chameleon model (f(R))

WMAP7 cosmology:

$$\{\Omega_{\rm m}, \Omega_\Lambda, n_{\rm s}, h \equiv H_0/(100{\rm km/s/Mpc}), \sigma_8\} = \{0.24, 0.76, 0.961, 0.73, 0.80\}$$

Models	$L_{\rm box}$ (h^{-1} Gpc)	Particles	Domain meshes	Finest meshes	Convergence criterion	Realizations
ΛCDM, F6, F5, F4	1.0	1024^3	1024^3	65536^3	$\|\epsilon\| < 10^{-12}/10^{-8}$	1
ΛCDM, F6, F5, F4	1.5	1024^3	1024^3	65536^3	$\|\epsilon\| < 10^{-12}/10^{-8}$	6

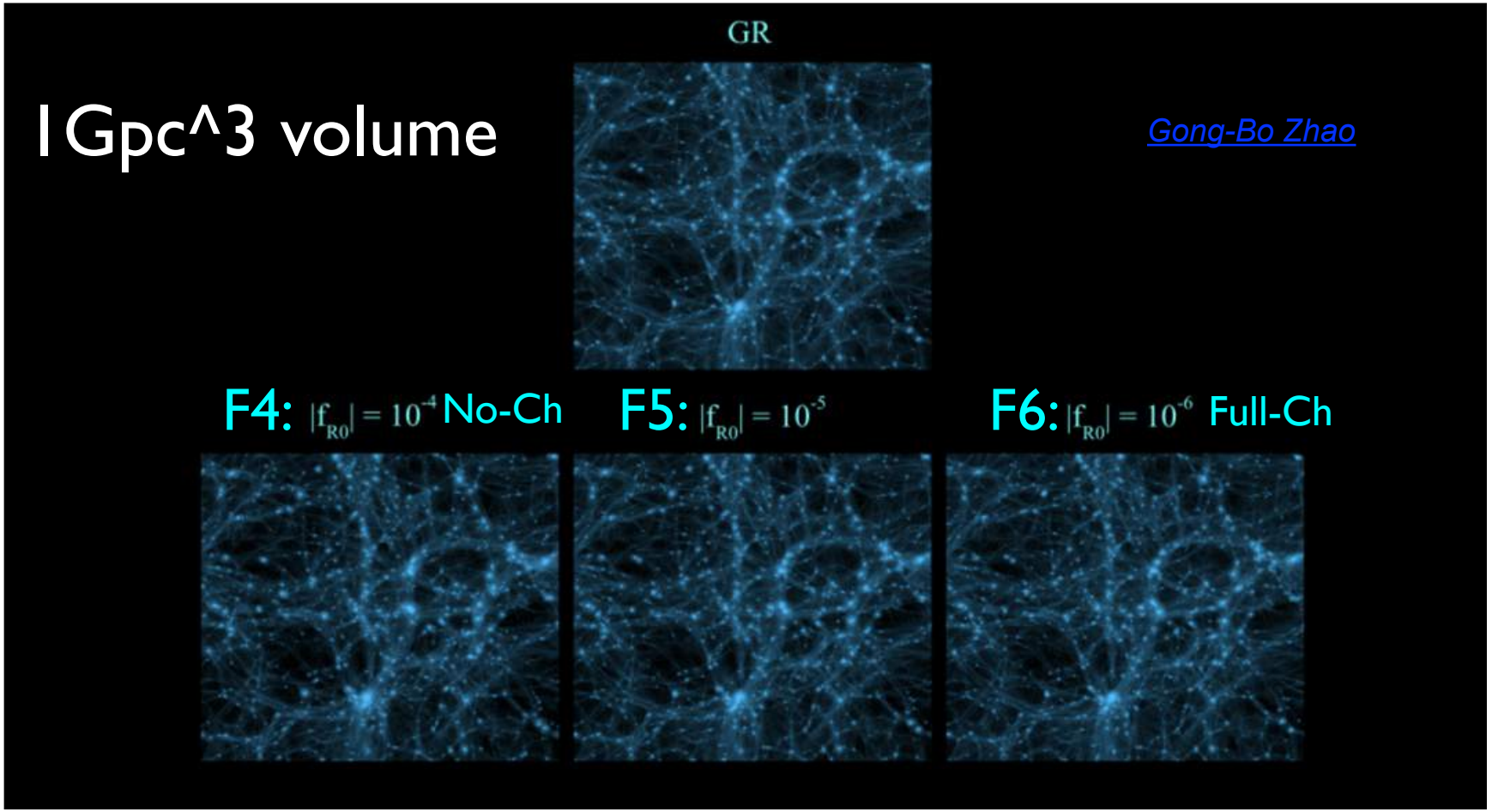

GR

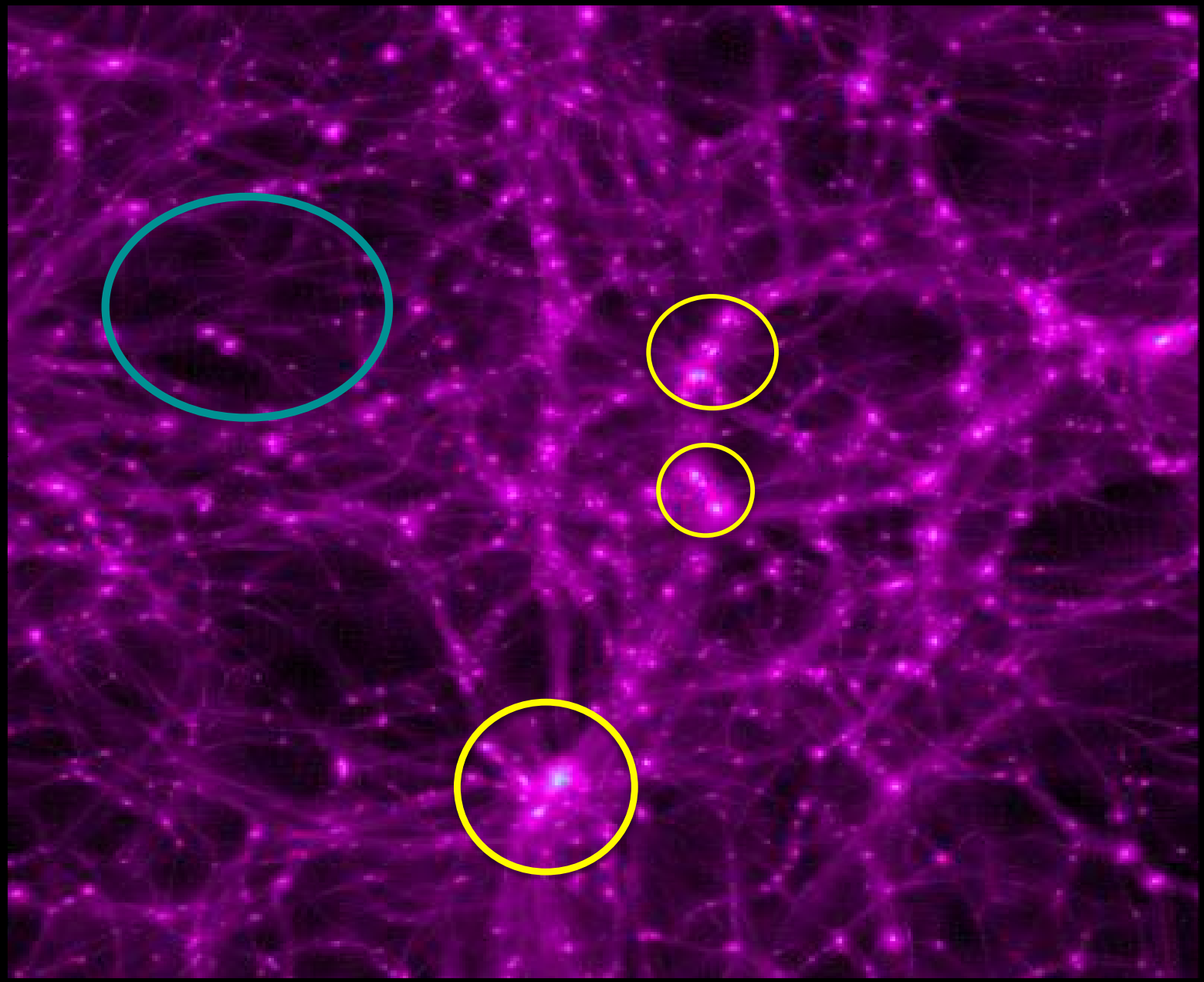

Gong-Bo Zhao

f(R)

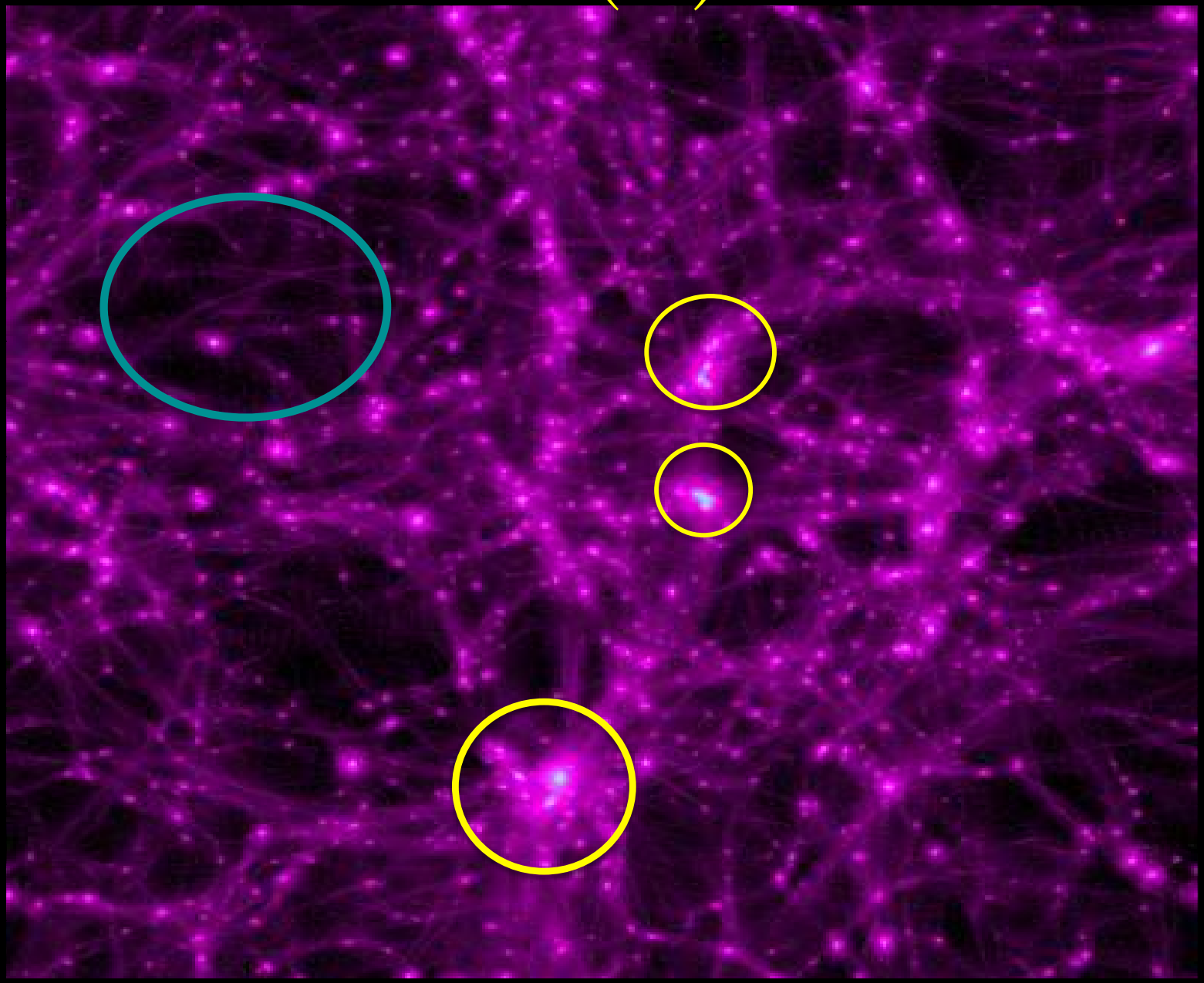

Gong-Bo Zhao

f(R) predictions using toy model

Haloes and the fifth force

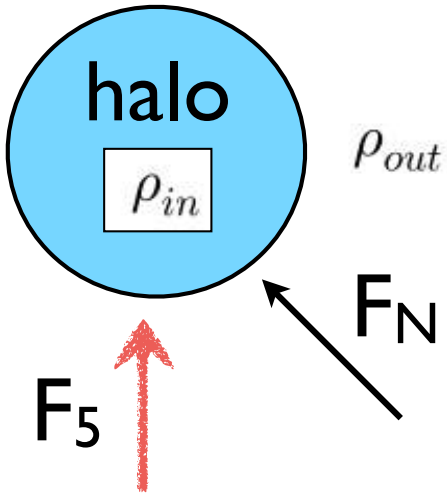

- Positive fifth force outside haloes acting in addition to newtonian.
- Effect present at low masses.
- At high masses effect increases for high fifth force strength parameter.

Full f(R) simulations

Mass functions:

Zhao, Li & Koyama, 2012

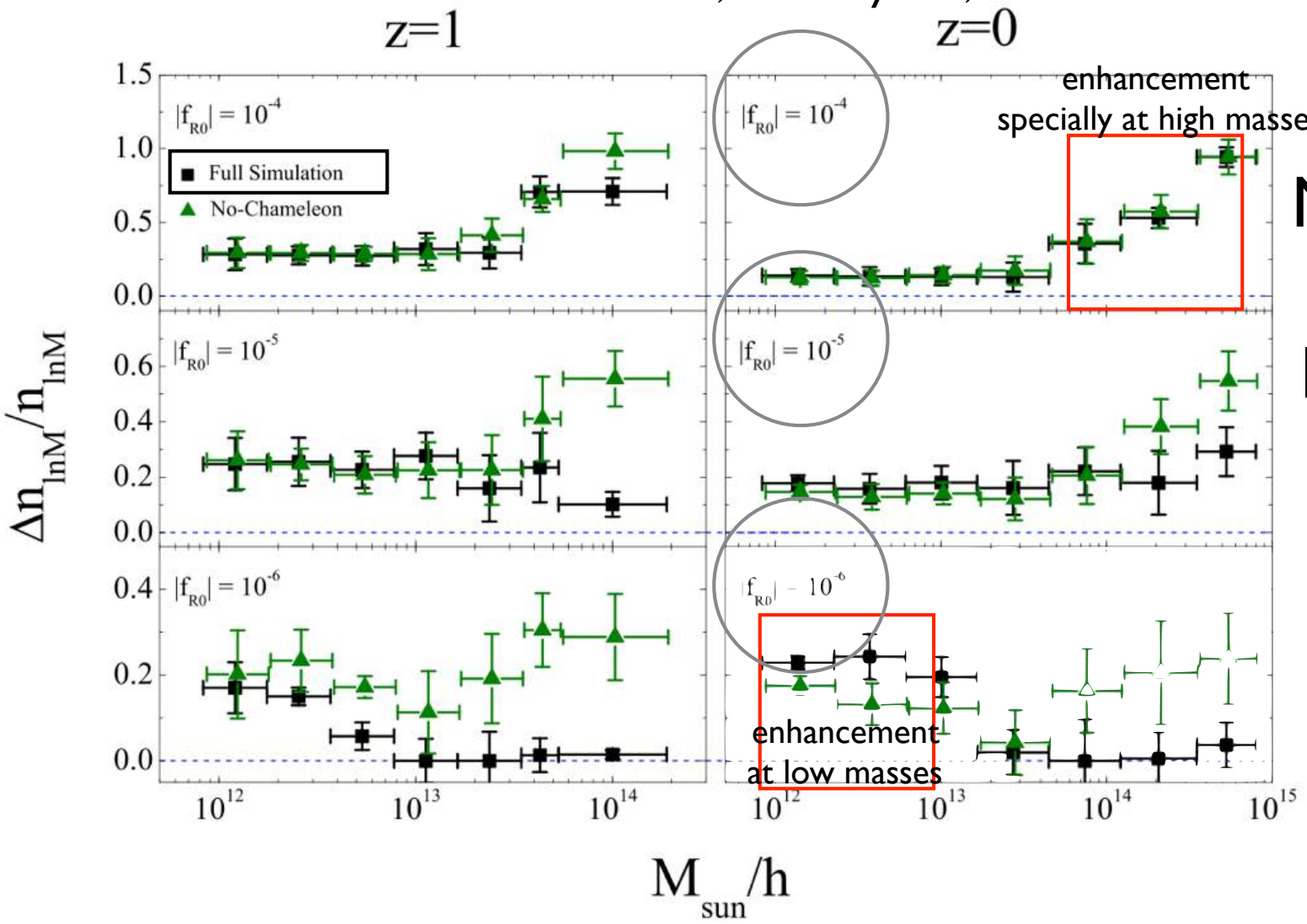

No screening

Intermediate screening

Full Chameleon

Full f(R) simulations

Power spectra:

Zhao, Li & Koyama, 2012

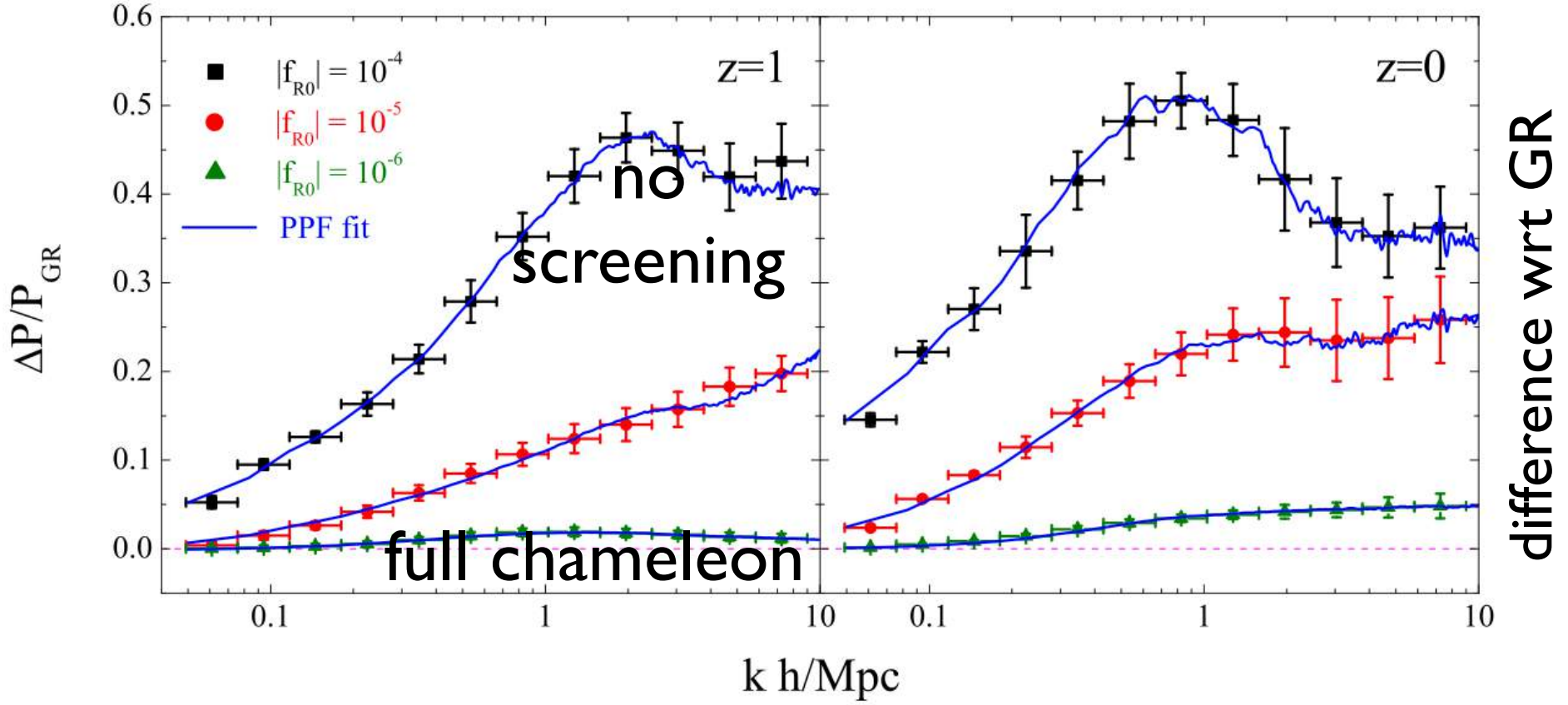

Clustering of mass is different; sigma_8 is higher in f(R).

Full Vainshtein screening simulations (nDGP): different mass functions, different mass P(k)

Diff. with GR: P(k)

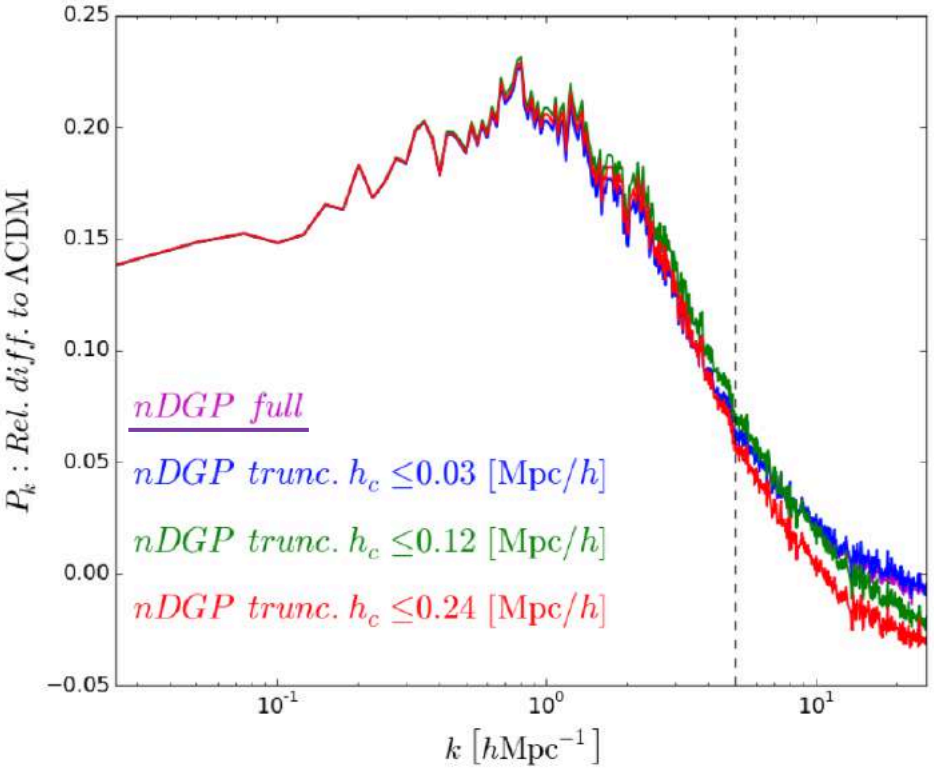

Diff. with GR: Mass Function

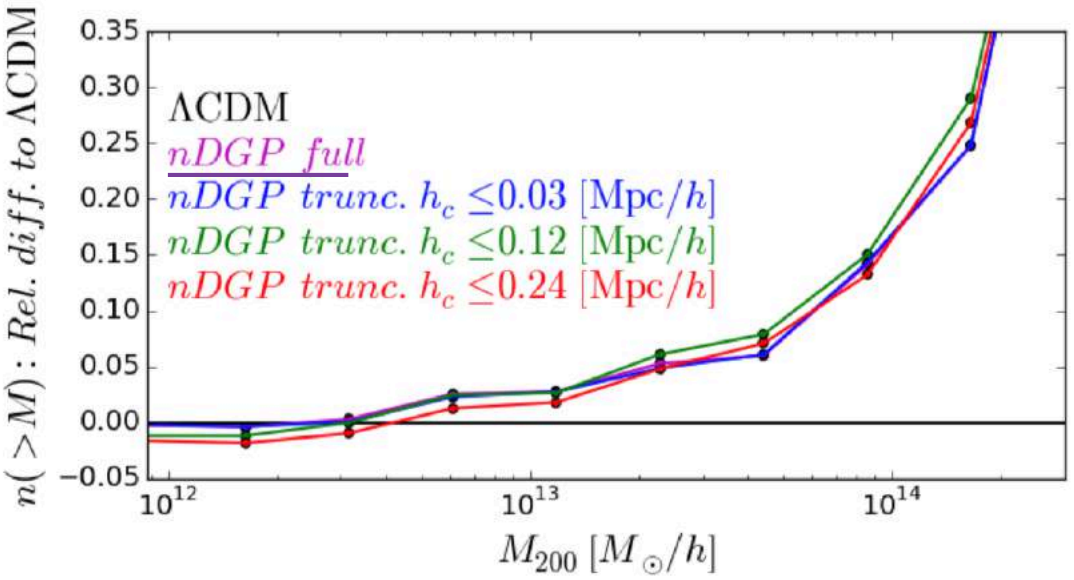

Clustering of mass is different; sigma_8 is higher in nDGP.

What can we do about galaxy clustering?

What is the Halo Occupation Distribution?

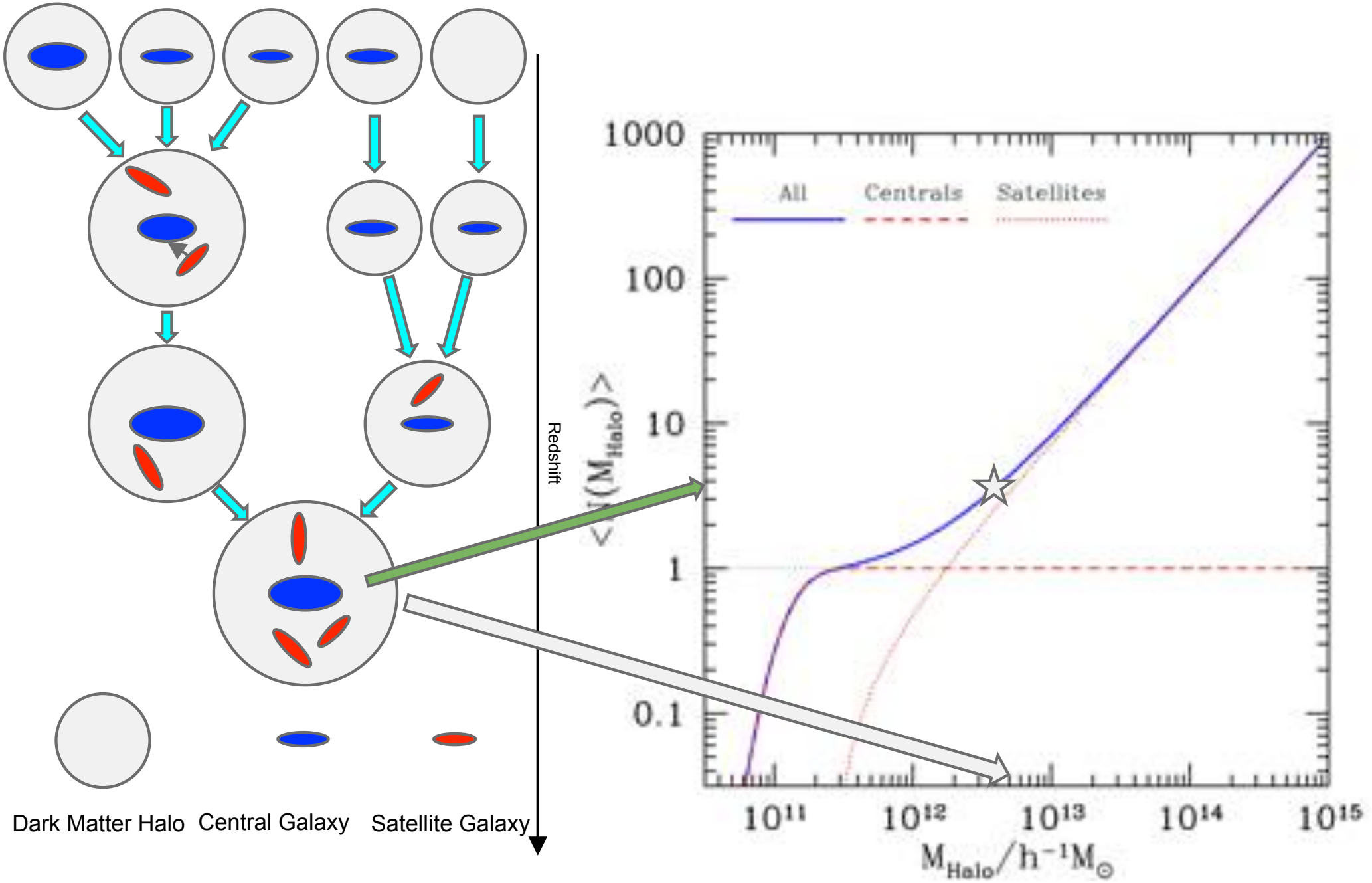

Galaxies instead of mass.

SHED I: Cautun+2018

Mass distribution is different in f(R) with respect to GR, but we must reproduce observed

(i) galaxy abundance,
(ii) galaxy clustering,
(iii) CMB.

Optimization of halo occupation model parameters until clustering is fit.

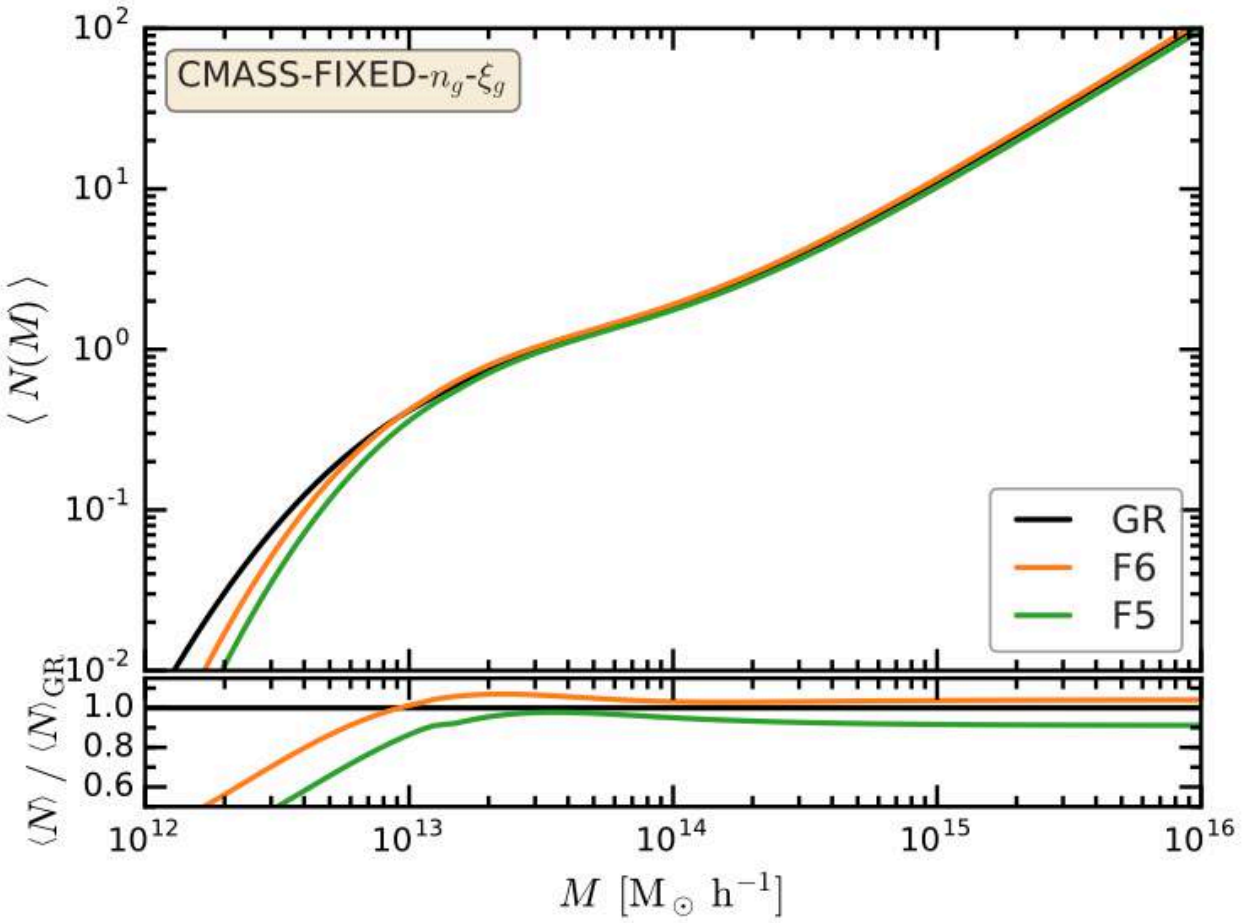

Cautun et al. 1710.01730

Implementation of gas and stellar components on ECOSMOG ongoing: Cataldi et al. in prep

- GR, f(R) and nDGP with the same CMB initial conditions

- GR, f(R) and nDGP with the same galaxy clustering.

What could be different between MoG and GR?

- Low density regions

- Mass density around tracers

Two proposed tests

- Marked correlation functions involving density and host halo mass
- Weak lensing profiles around voids

Two proposed tests

- Marked correlation functions involving density and host halo mass
- Weak lensing profiles around voids

Even though galaxies show the same clustering, the distributions of local densities (Voronoi) and host halo masses differ.

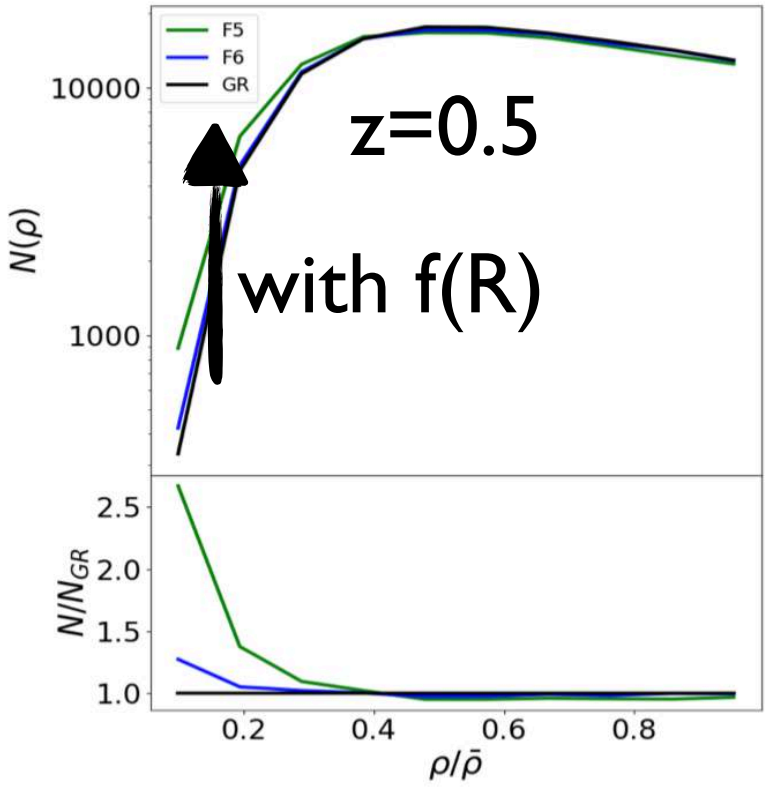

Figure 2. Distribution of galaxy local densities estimated using a Voronoi tessellation method. Only the range of below the mean density is shown for better illustration.

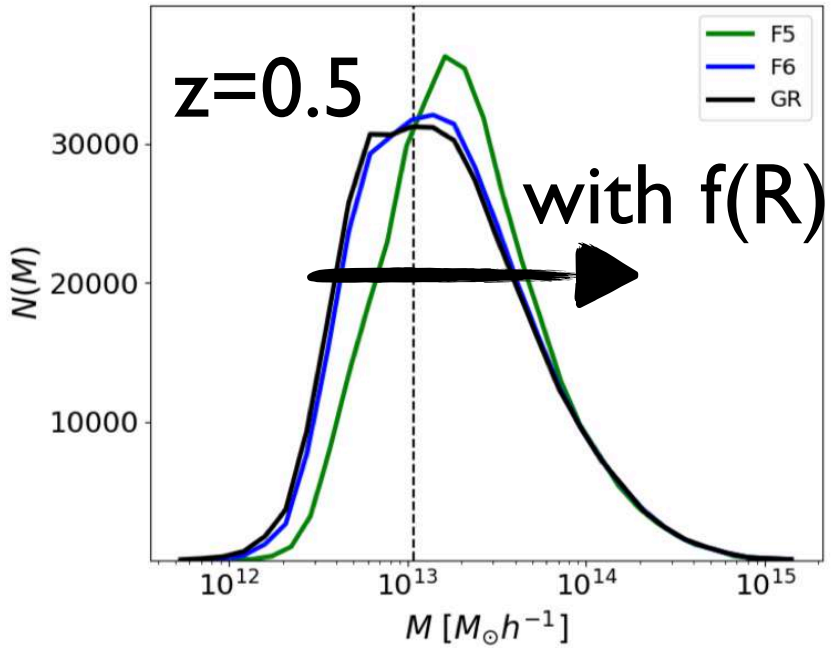

Figure 1. The distribution of the host halo mass M sampled by the HOD galaxies for different models as labelled in the legend. The dashed line indicates mean value for GR.

Armijo et al. 1801.08975

Marked Correlations

$$\mathcal{M}(r) = \frac{1}{n(r)\bar{m}^2} \sum_{ij} m_i m_j, \quad m_i = M_i^p$$

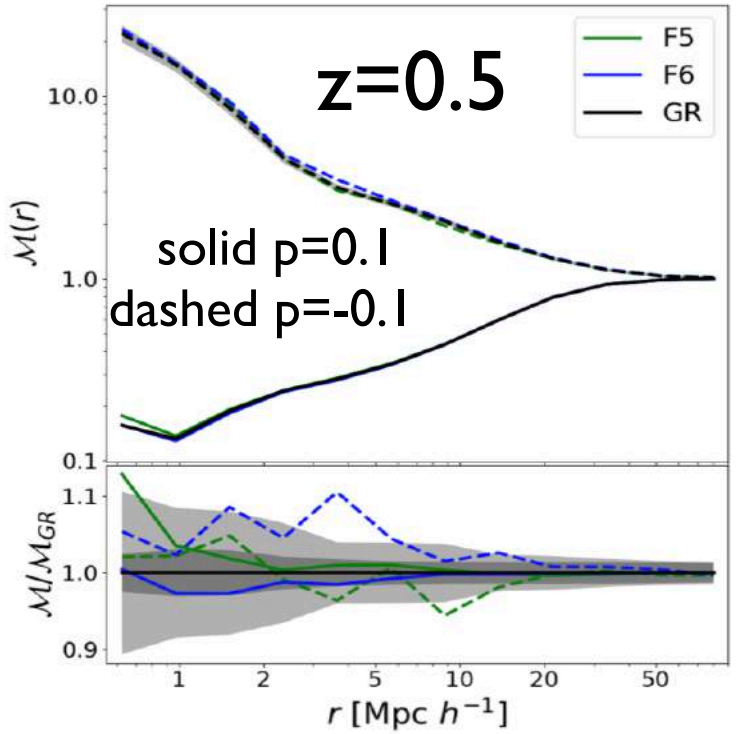

Figure 3. The marked correlation function $\mathcal{M}(r)$ using the local density ρ as the mark. This plot shows the examples for $\mathcal{M} = \rho^p$, with $p = \pm 0.5$ in solid (-0.5) and dashed lines (0.5). The lower panel shows the ratios of marked correlation functions between $f(R)$ and GR. The shaded regions correspond to the errors on the mean corresponding to a volume of $\sim 1(h^{-1}\mathrm{Gpc})^3$ estimated using the Jackknife method. The dark and light shaded regions are for the case of $p = -0.5$ and $p = 0.5$ respectively.

For the case of M_i=density, there is little difference.

M(r)=1, on average the product of marks is equal to the average.

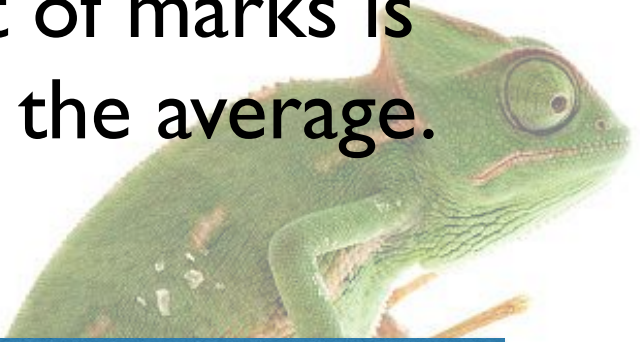

Armijo et al. 1801.08975

Mark=host halo mass

Armijo et al. 1801.08975

F5 shows significant differences in all cases

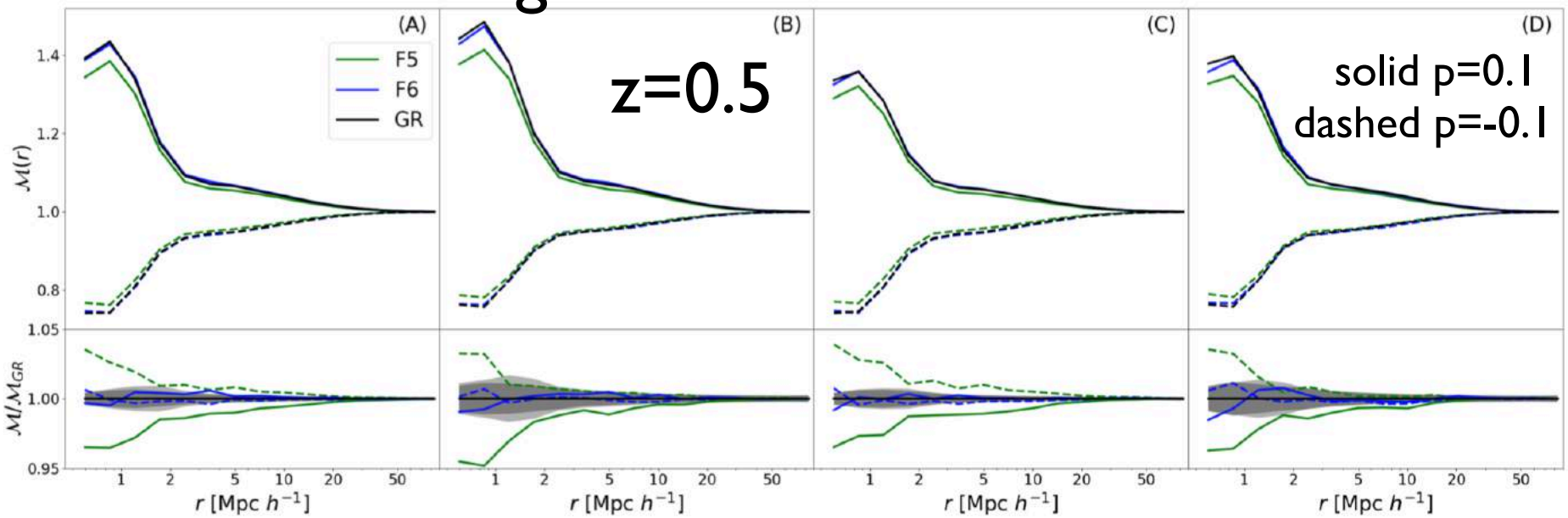

host mass with 0.1dex scatter

host mass with 0.2dex scatter

Stacking of WL for gx in 8 bins of Mstellar

Stacking of WL for gx in 8 bins of Mstellar scatter 0.2dex

Closer to what can be done with observations

Two proposed tests

- Marked correlation functions involving density and host halo mass
- Weak lensing profiles around voids

SHED I: chameleon Cautun+18
SHED II: chameleon vs. Vainshtein Paillas+19

7 Different void finders, 4 3D finders, 3 void finders in 2D

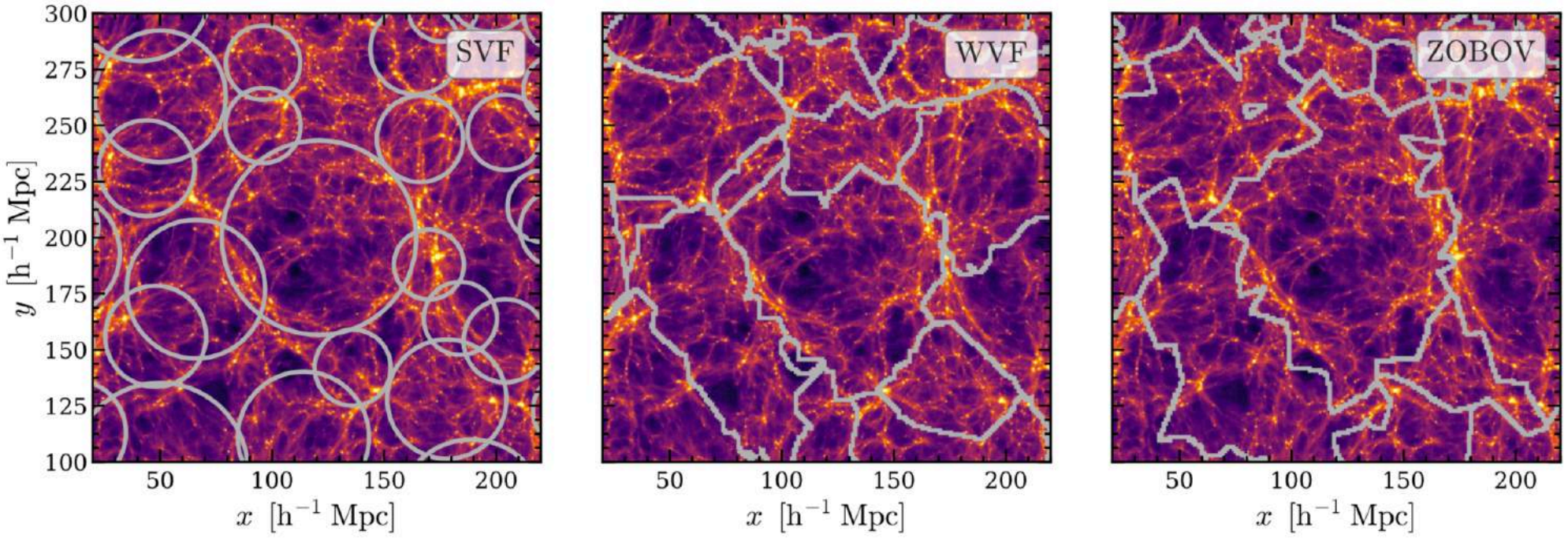

Cautun et al. 1710.01730 Paillas+1810.02864

Void finder list:

- Spherical void finder (NP+06)
- Watershed void finder (Platen+07)
- ZOBOV finder (Neyrinck 08)
- Watershed walls (Cautun+16)

3D

- Spherical 2D void finder (Cautun+18)
- 2D Tunnels, regions with no gals (Cautun+18)
- Troughs, fixed radius, 2gals (Gruen+16)

2D

2D vs. 3D finders

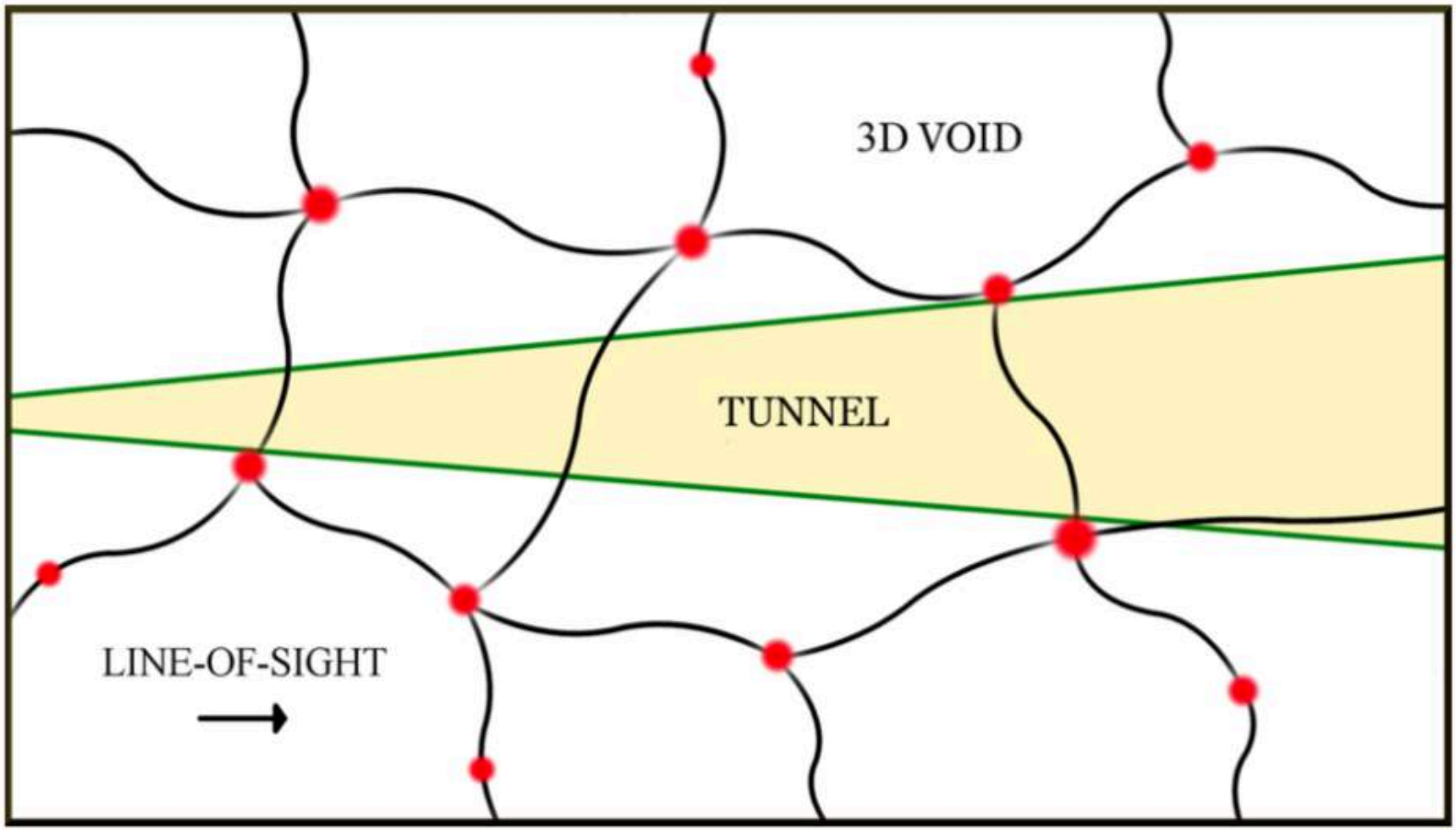

Paillas+1810.02864

Recap: f(R) predictions using spherical top-hat model

- Clampitt et al. 2013 calculate the fifth and newtonian forces for a top-hat empty region (**voids**).

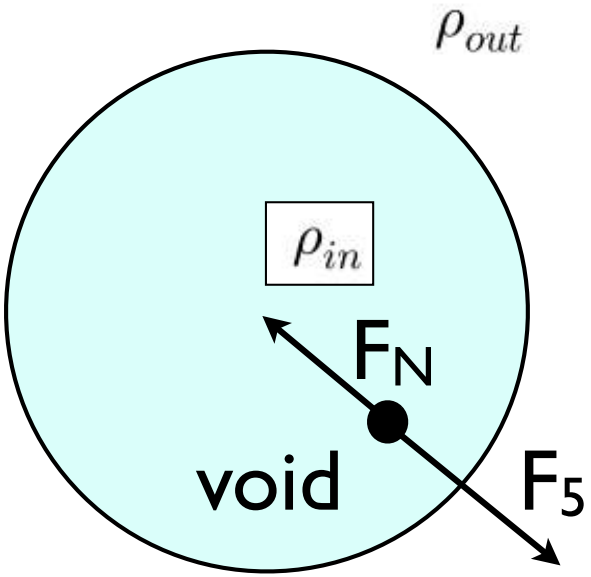

Negative fifth force inside voids acting in opposite direct-ion to newtonian. Stronger for lower internal density, and for small voids.

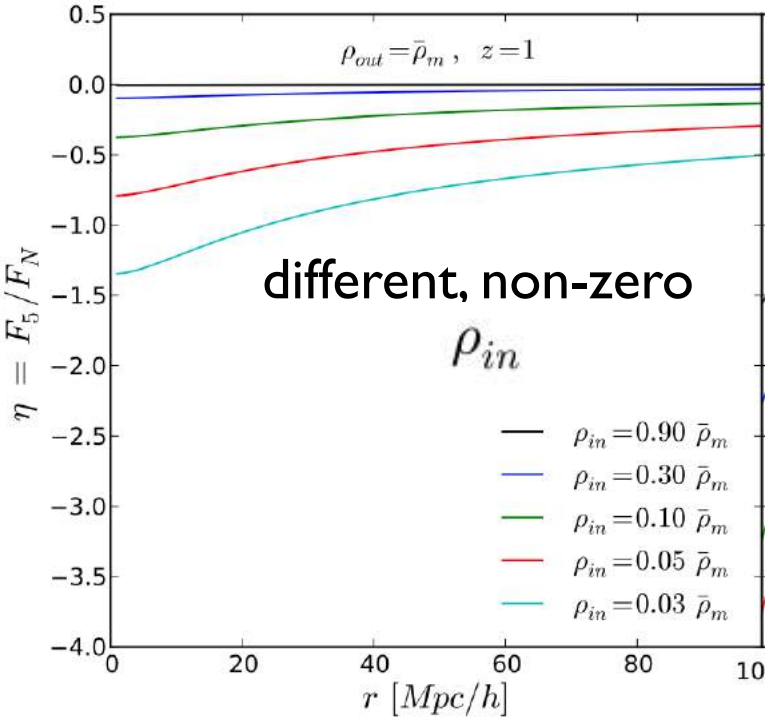

Void abundances (mass)

mP05 void abundances in the mass in f(R) simulations and GR.

25% difference between F6 and GR (highly significant), and up to x3 factor for F4.
Practical difficulties to measure.

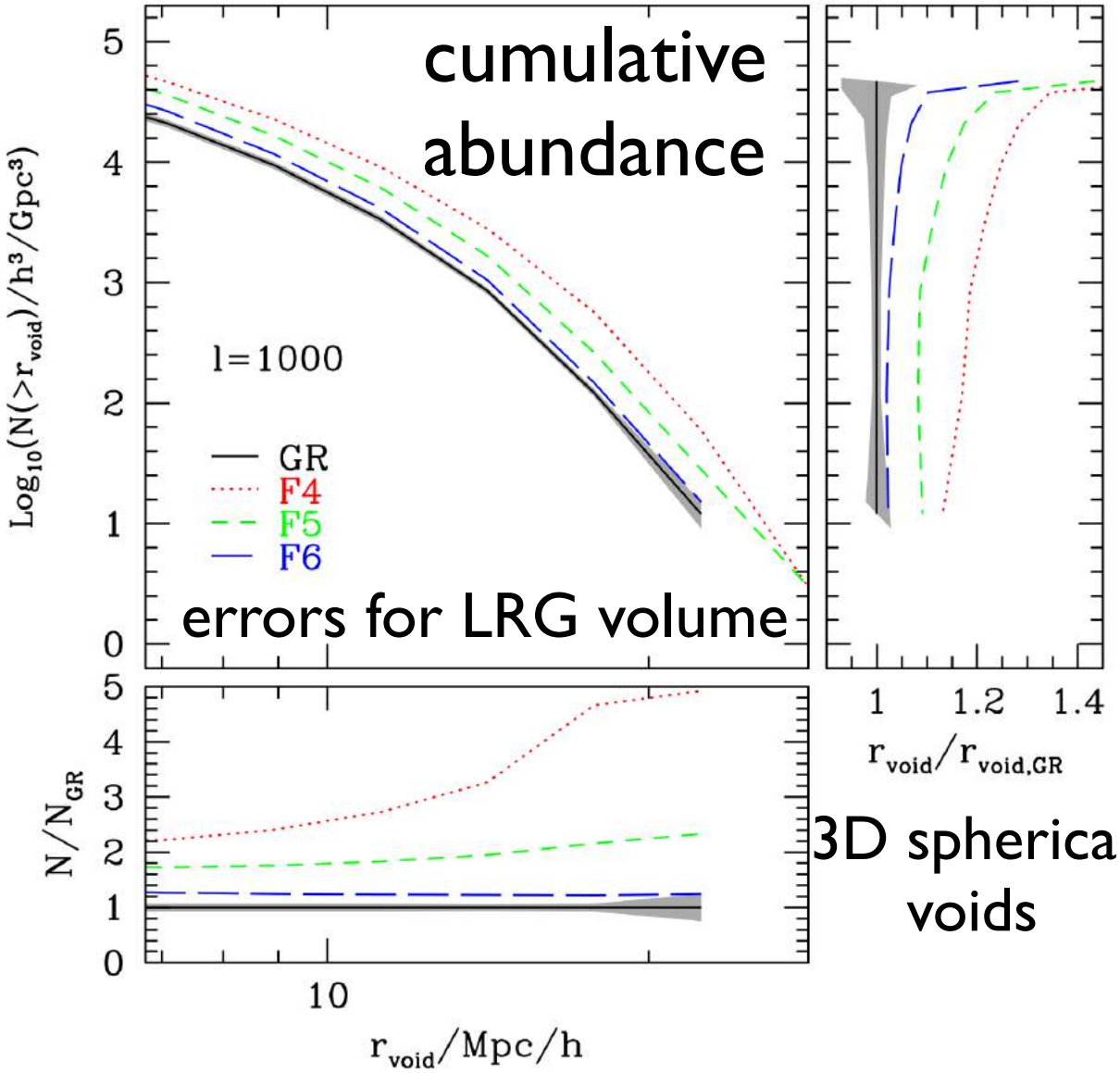

Cai, Padilla, Li, arXiv:1410.1510, see also Zivick et al., 2015

Void abundances (GALAXIES)

Spherical and Watershed void abundances in f(R) and nDGP simulations and GR, using CMASS volume, clustering and space density.

Differences are simply not there (no more info than in correlation function).

Cautun et al. 1710.01730
Paillas+1810.02864

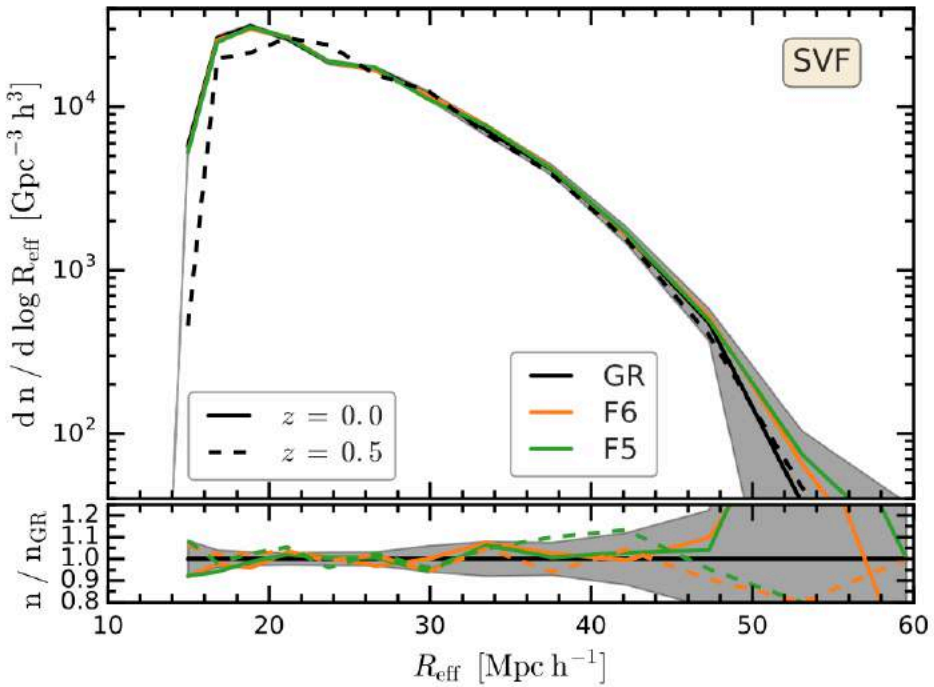

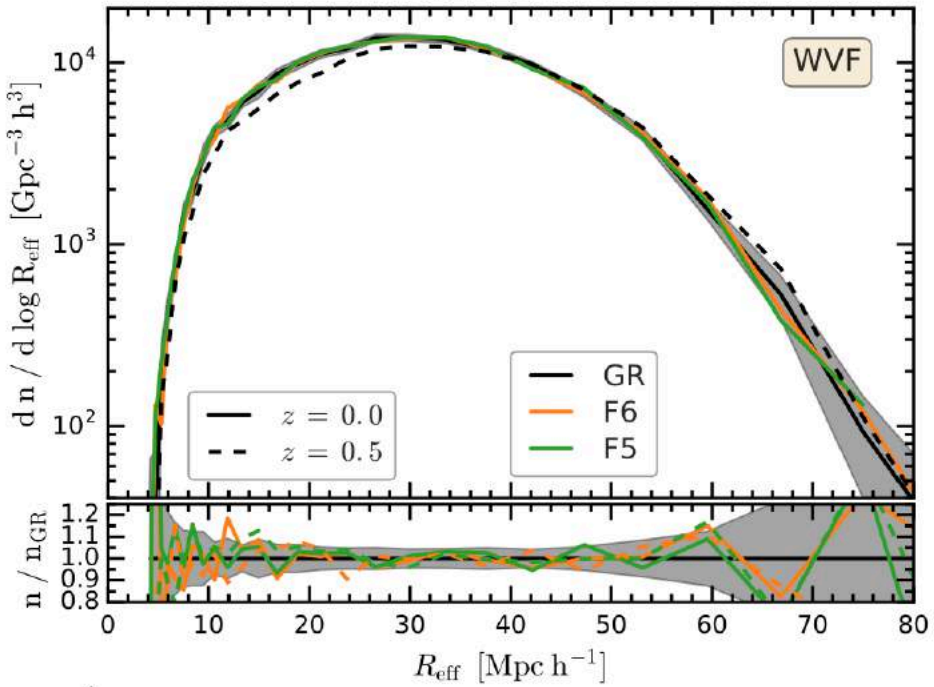

Testing gravity with cosmic voids

Cai, Taylor, Peacock, NP, 2016, MNRAS, 462, 2465

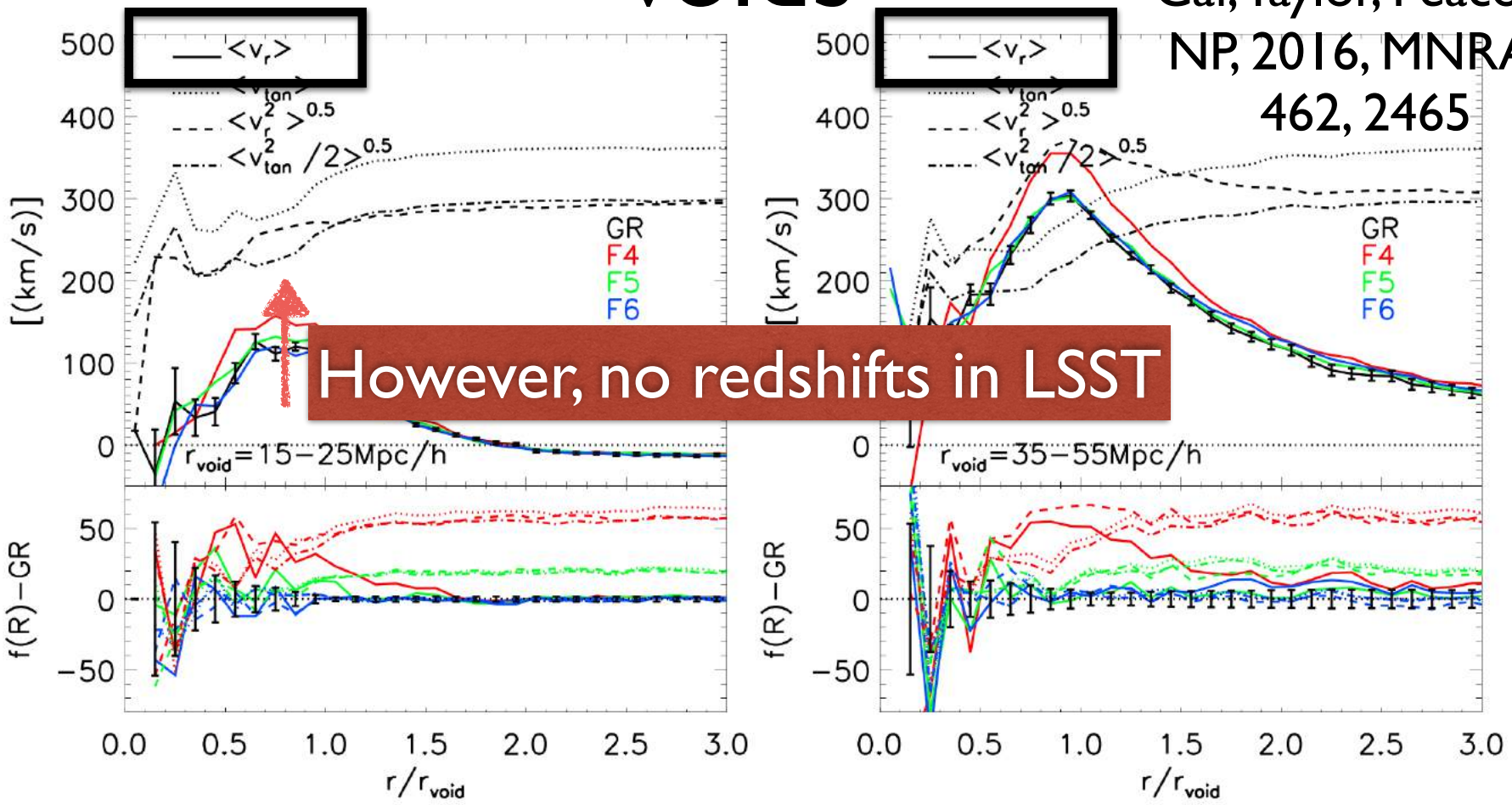

Voids expand ~10-50km/s faster in f(R) (test done with 1 Gpc/h a side volume)

SHED I, see also Li et al. 2016, Song et al. 2016, Chaung et al. 2016

Paillas et al. (2016): effects of baryons ~5km/s

Stacked void profiles

Differential profiles traced by galaxies.

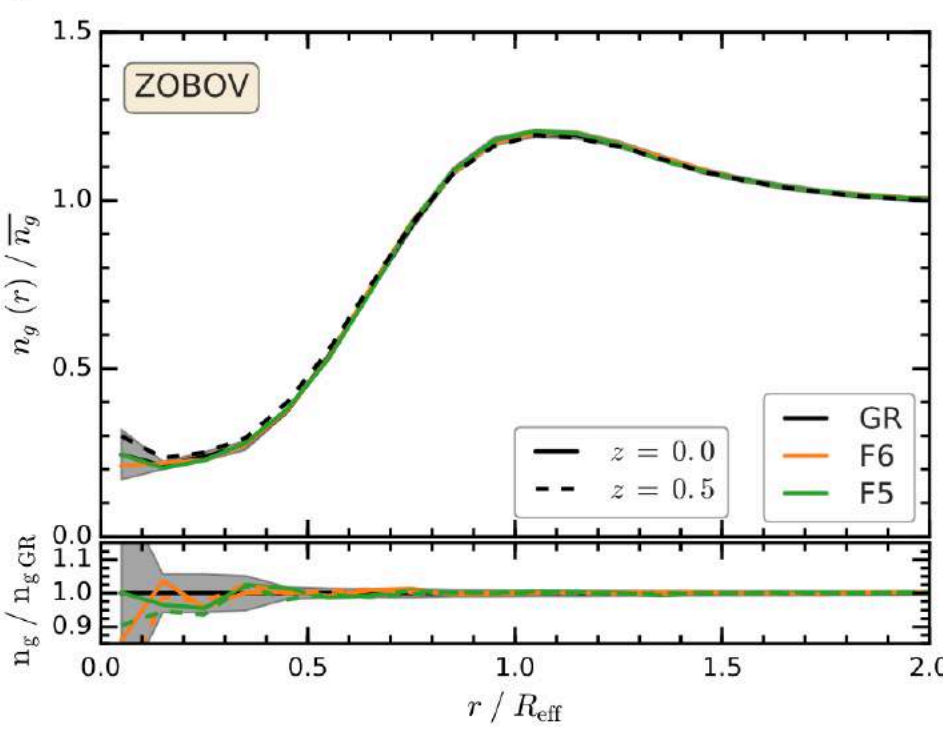

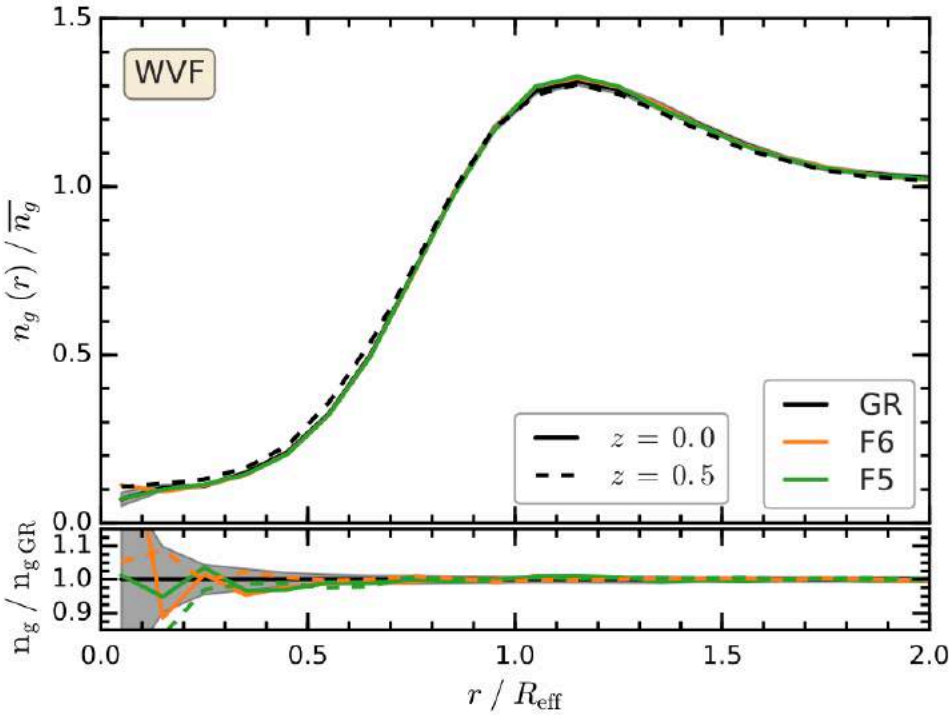

Because galaxy clustering is the same, the stacked profiles only show mild differences in f(R) (also nDGP)

Cautun et al. 1710.01730

Stacked void profiles

Differential profiles traced by mass.

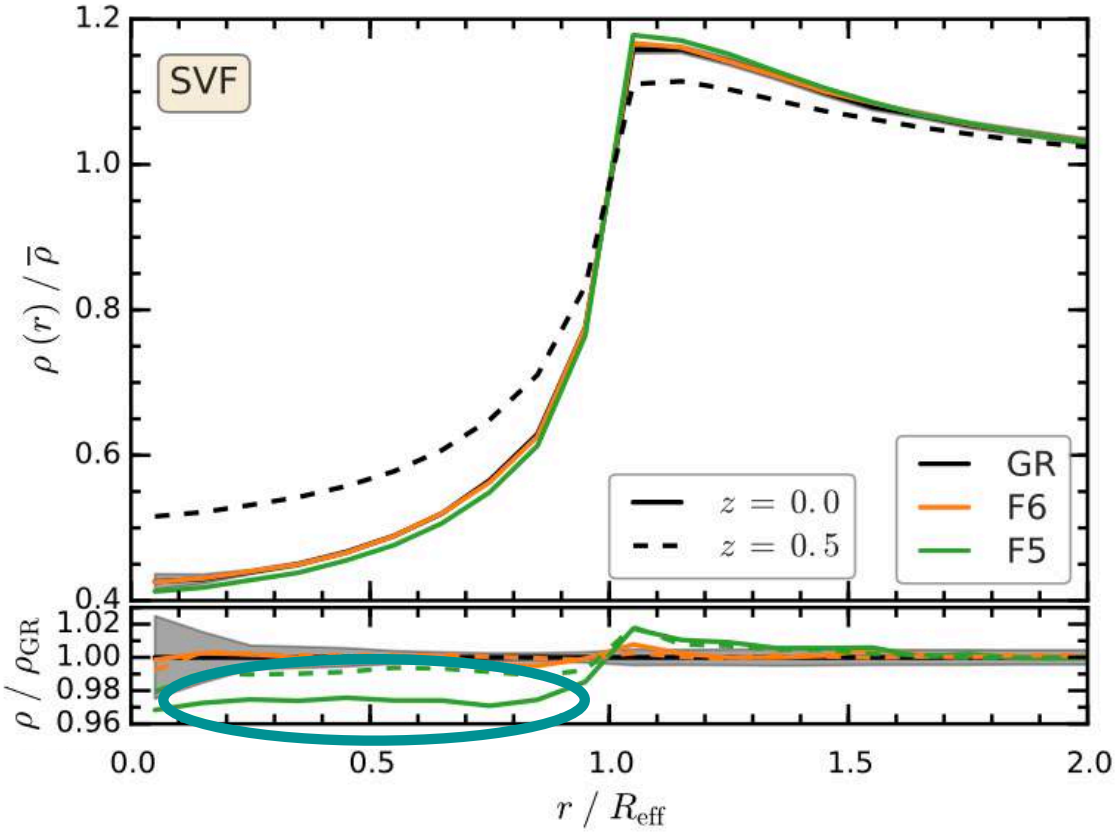

DM profiles confirm emptier voids in f(R) models even if galaxy clustering, void abundances and galaxy profiles are the same. Similar results for nDGP (Paillas+19)

Cautun et al. 1710.01730

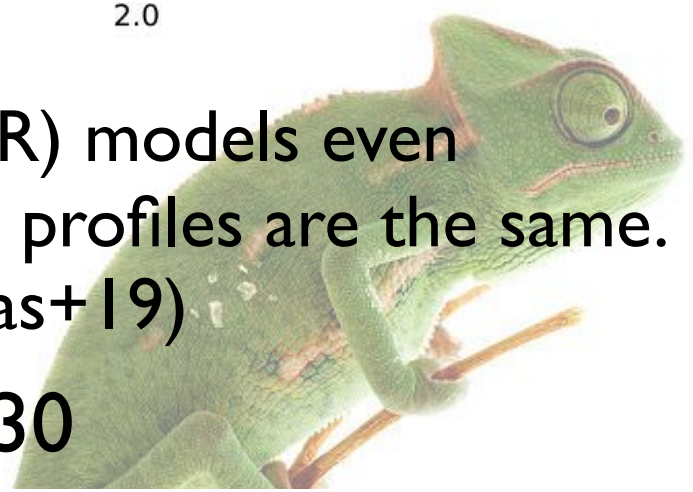

Weak lensing shear profiles

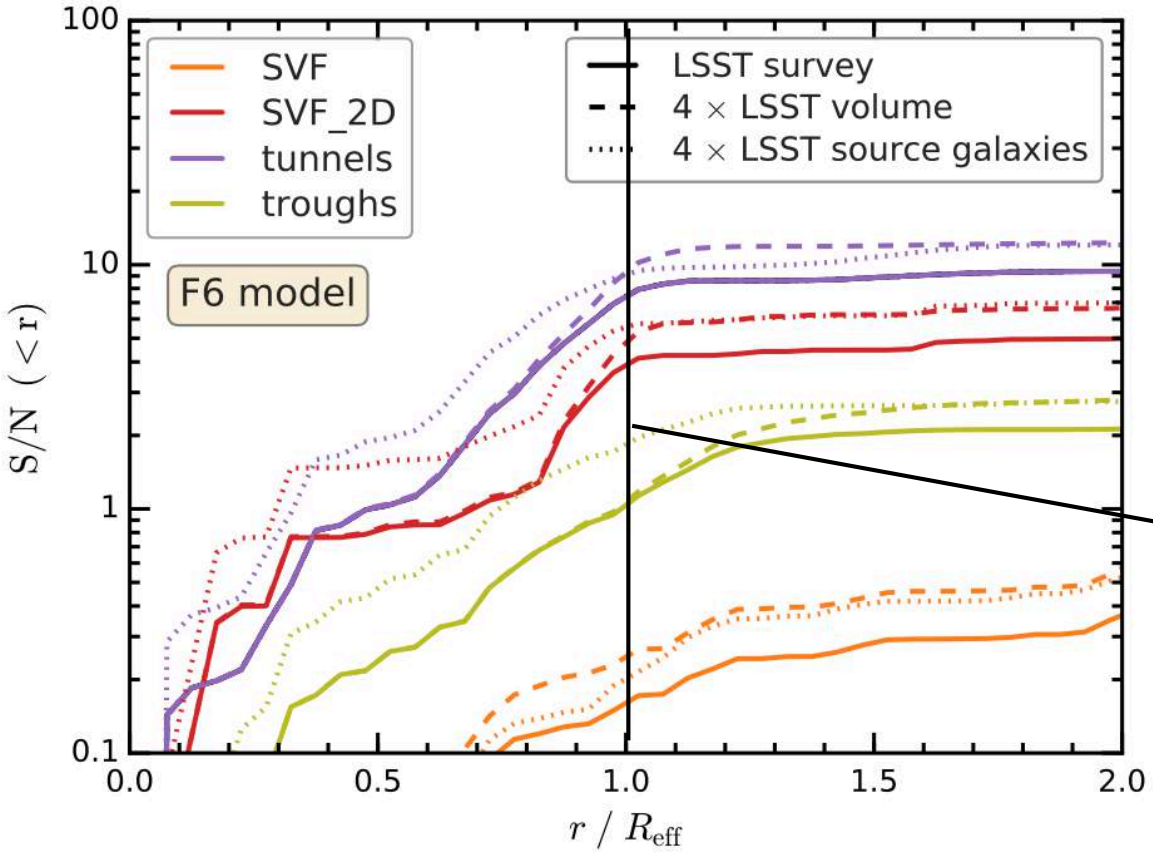

S/N quoted at Reff

Lensing can be used to detect f(R) with LSST (or DESI)
Especially with 2D finders

Cautun et al. 1710.01730

Paillas et al. 2018: host haloes of tunnels are different in chameleon and Vainshtein sims for equal galaxy clustering

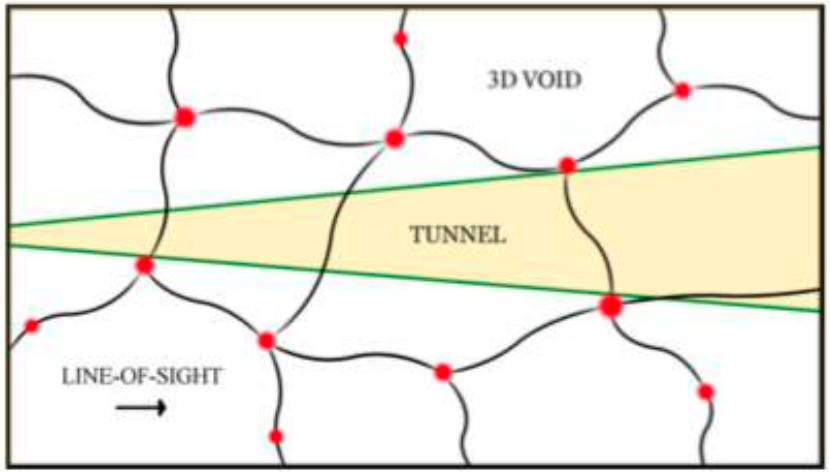

N1 and F5 with equal sigma_8

Effect on significance of differences with respect to GR on 2D voids.

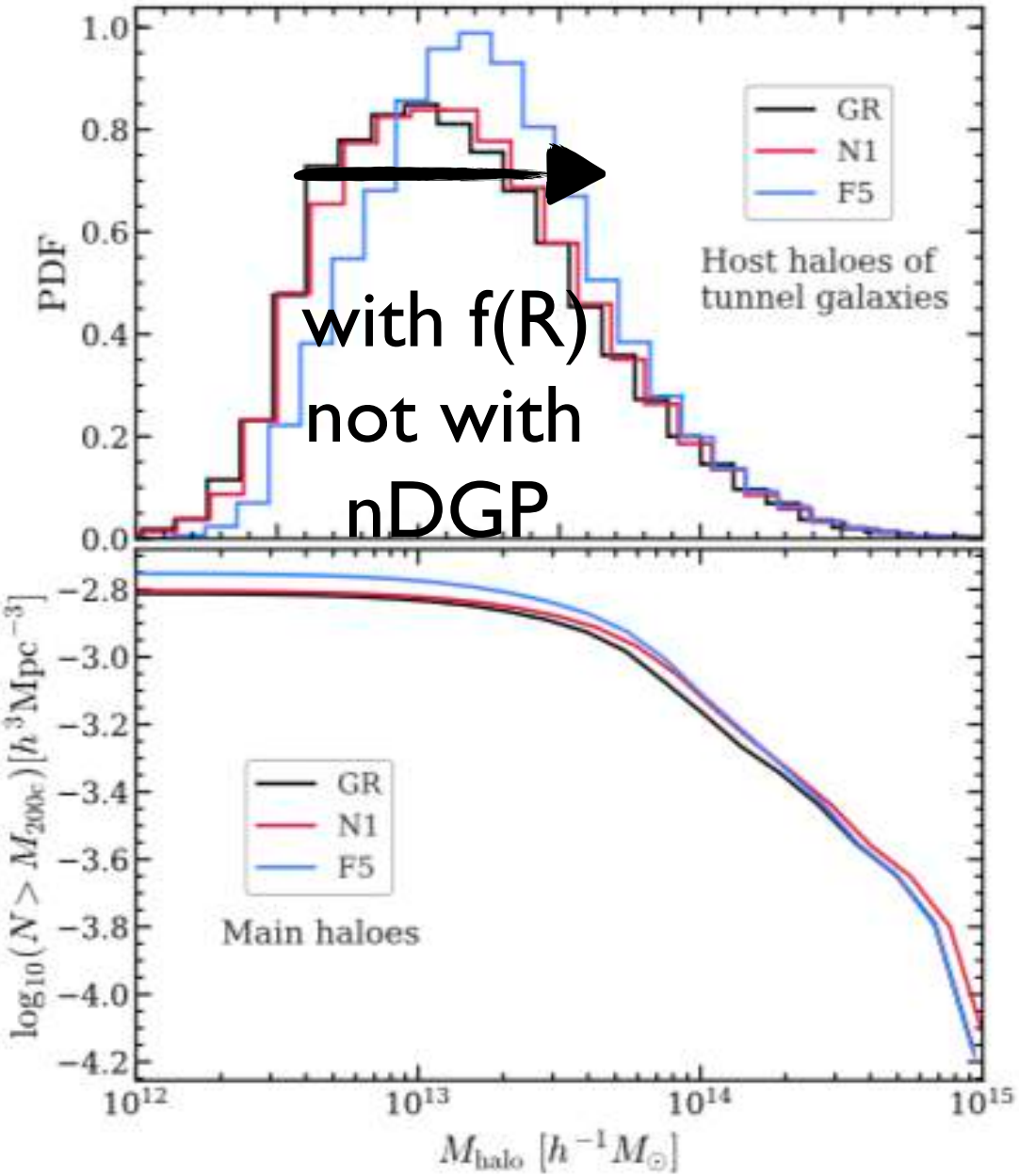

Paillas et al. 2018: host haloes of tunnels are different in chameleon and Vainshtein sims for equal galaxy clustering

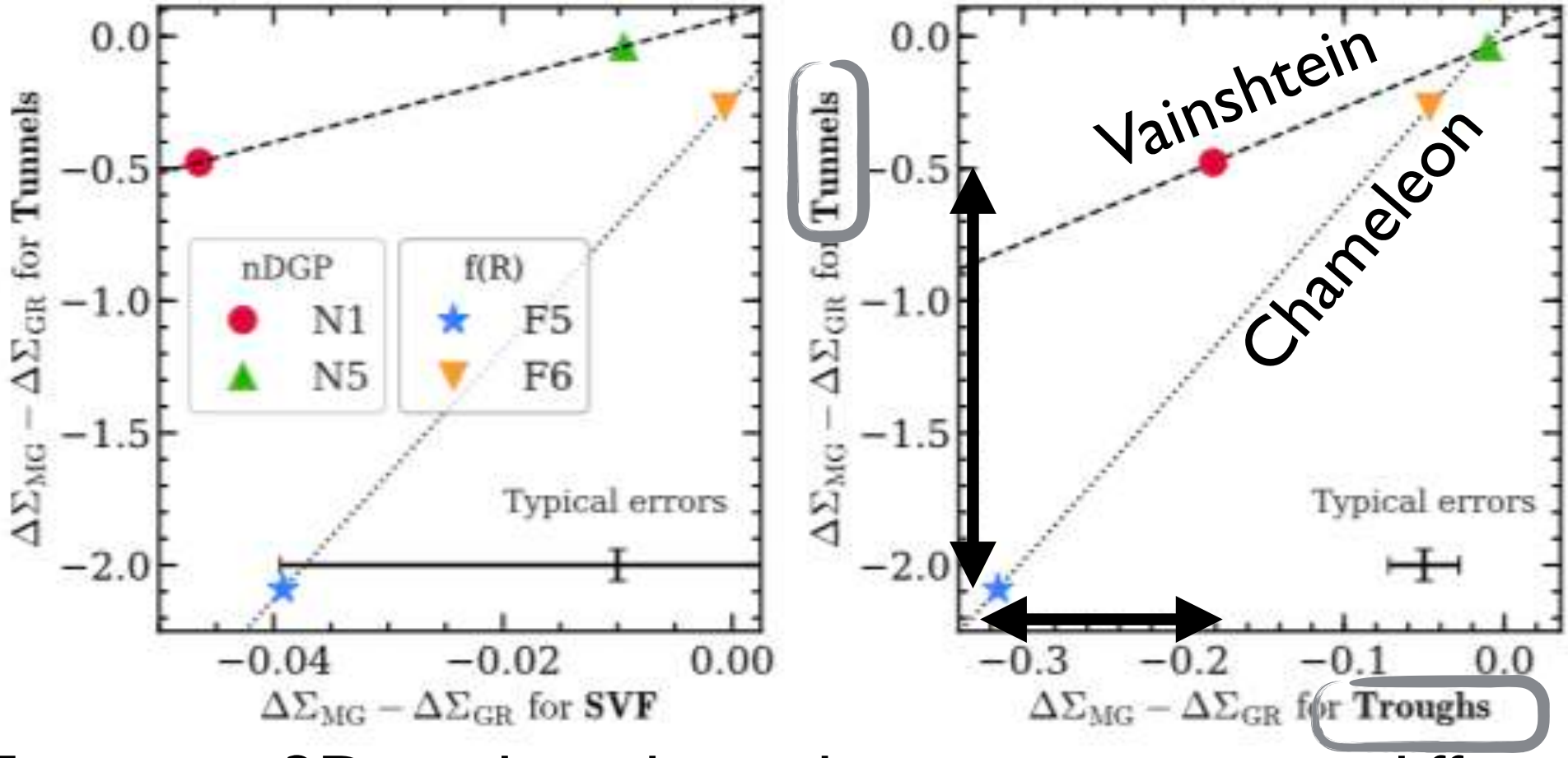

Errors on 3D voids makes it better to compare different 2D void finders.

Chameleon is way farther away from GR than Vainshtein for 2D voids

Conclusions

- Voids found using galaxies: abundances and galaxy density profiles indistinguishable.
- GR, nDGP and f(R) galaxies with equal clustering would have different halo masses and mass density profiles around galaxies, and voids.
- Marked correlation functions can enhance differences seen in 1-point functions in a statistical way.
- RSD tests can help detect departures from GR (DESI).
- Comparison of difference between WL around different types of 2D voids wrt GR exposes screening mechanisms with LSST.

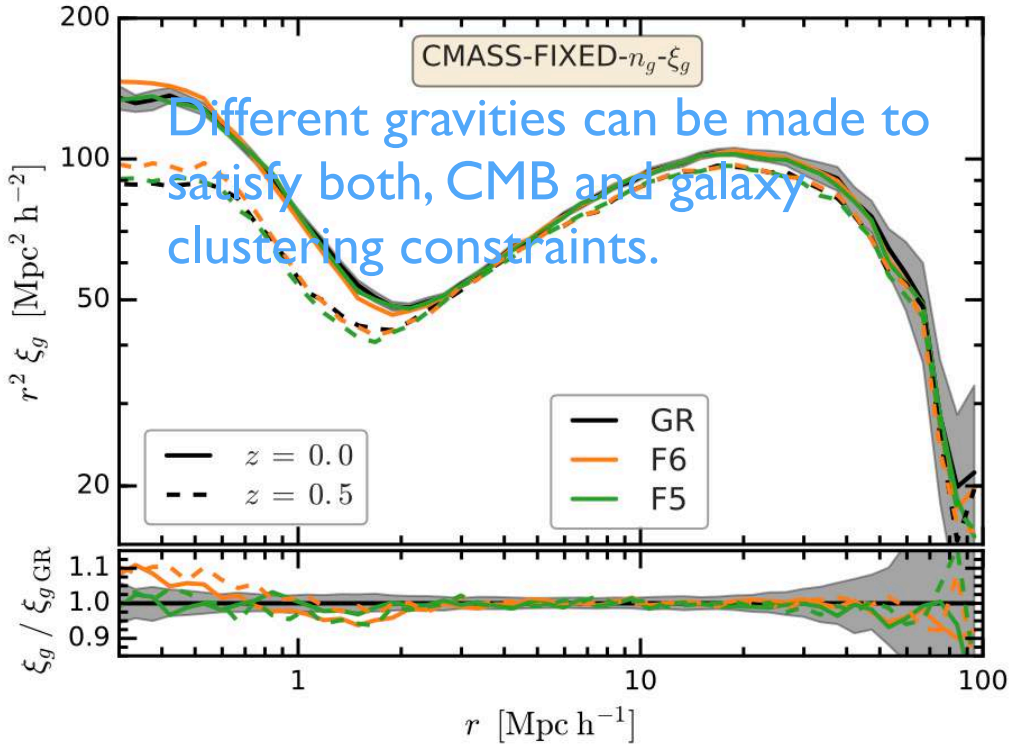

Cai, NP, Li 2015, MNRAS, 451, 1036
Cai, Taylor, Peacock, NP, 2016, MNRAS, 462, 2465
Armijo, Cai, NP, Li, 1801.08975
Cautun et al., 2018, MNRAS, 476, 3195
Paillas et al. 1810.02864

AIUC
CENTRO DE ASTRO-INGENIERIA UC